# Chapter 2

# Synthesis, Antimicrobial Activity and *In Silico* Studies of Benzoxazole-Piperazine Hybrids Amide Linkages

## 2.1 Introduction

The heterocyclic molecule benzoxazole is composed of a fused benzene and oxazole ring system. Due to its planar and electron-rich structure, it exhibits significant pharmacological flexibility.[54] The resultant hybrid compounds frequently show increased bioavailability, higher solubility, and strong binding affinity to biological targets with the piperazine moiety.[55] The creation of new medicinal compounds with promise antibacterial,[56] antifungal,[57] anti-inflammatory,[58] anticancer,[59] and CNS-modulating qualities has resulted from this structural combination.[60]

Benzoxazole derivatives containing piperazine have garnered considerable attention in medicinal chemistry due to their diverse range of biological activities and potential therapeutic applications.[61] The addition of piperazine units to benzoxazole scaffolds has been shown in several investigations to impact the final products pharmacokinetic and pharmacodynamic characteristics substantially.[62] In the case of CNS-active medication design, for example, piperazine derivatives are particularly appealing due to their recognized capacity to interact with a variety of neurotransmitter receptors and enzymes.[63] Consequently, benzoxazole derivatives containing piperazine have been investigated for use in anticancer, antifungal, and neuroprotective medications, demonstrating their promise as lead molecules in drug development.[64]

Many common antibiotics are no longer effective due to the emergence of resistant strains of pathogens such *S. aureus*, *E. coli*, *B. subtilis*, *P. aeruginosa*, *A. niger*, and *C. albicans*.[65] This highlights the critical need for new therapeutic medicines.[66] As antibiotic and antimicrobial agent resistance, especially in gram-positive bacteria, poses serious problems for the healthcare and agricultural sectors, new medication classes are desperately needed.[67] The distinct structural and electrical characteristics of benzoxazole derivatives have attracted a lot of interest in drug development because they allow for a variety of biological functions.

A fundamental component of medicinal chemistry, amide bonds play a crucial role in enhancing the physicochemical characteristics of bioactive compounds.[68] They are

essential in hybrid drug design because they improve metabolic stability, molecular stiffness, and hydrogen-bonding interactions with biological targets.[69] The antibacterial activity of amide linkages has also been shown to be enhanced by better binding interactions with bacterial proteins.[70]

Benzoxazole and piperazine frameworks joined by amide bonds are combined in hybrid compounds, which are intended to take use of each compound's distinct pharmacological characteristics.[71] The amide bond guarantees the hybrid molecule's structural integrity while encouraging robust microbial target engagement, piperazine optimizes pharmacokinetics and promotes multi-target interactions, and benzoxazole improves specificity and binding affinity.[72] The derivatives of the benzoxazole-piperazine combination provide a potential strategy by focusing on many microbial cell processes.[7] It has been demonstrated that this multi-target strategy reduces the probability of resistance development while retaining effectiveness against resistant strains.[74]

Numerous widely accessible drugs that include benzoxazole heterocycle show how important its derivatives are for creating novel compounds that may be used as medicinal agents.[75] Benzoxazole and piperazine are regarded as important biological active moieties with a variety of biological properties, such as anti-inflammatory (Flunoxaprofen, **1**),[76] (Benoxaprofen, **2**),[77] anti-psychotic (Salvianen, **3**),[78] anti-tubercular (Pseudopteroxazole, **4**),[79] nerve sparing agent (Tafamidis, **5**),[80] anti-cancer (Imatinib, **6**),[81] anti-psychotic (Aripiprazole, **7**),[82] CNS depressants (Eszopiclone, **8**),[83] Phosphodiesterase-5 (PDE5) inhibitor (Sildenafil, **9**),[84] anti-cancer (Quetiapine, **10**)[85] (**Figure 1**), underscoring these frameworks' adaptability in drug creation.

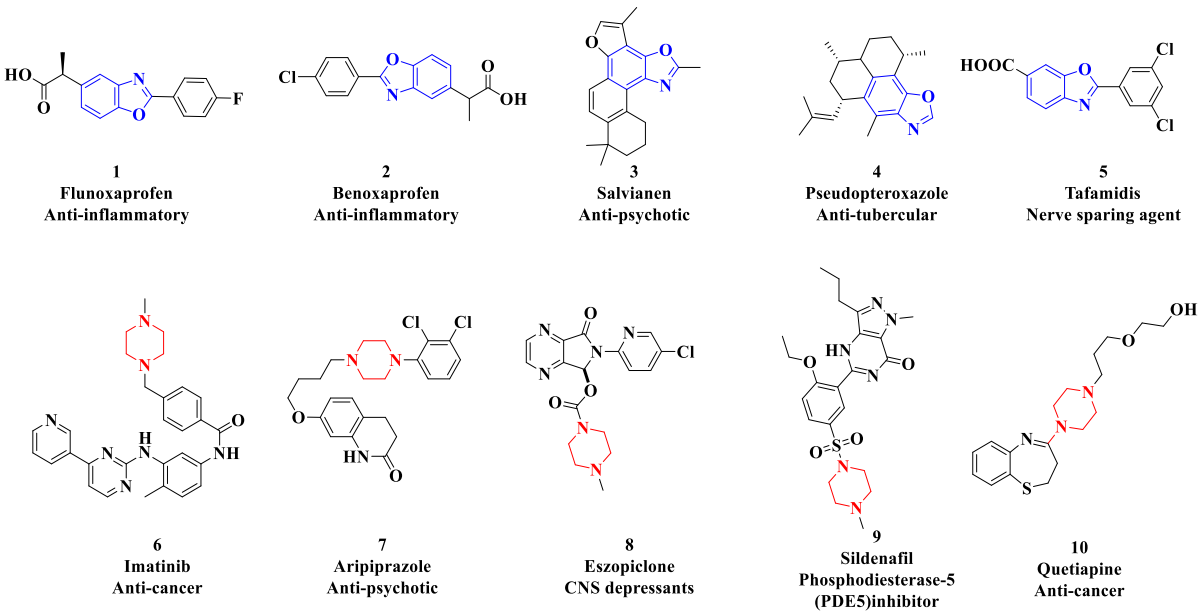


**Figure 1:** Marketed drugs containing Benzoxazole and piperazine motifs.

### 2.1.1 Synthetic methodologies for the substituted benzoxazole and piperazine framework and its biological significance

To a solution of 2-amino-4-chlorophenol (**11**) in ethyl acetate, substituted phenylisothiocyanate (**12**) and copper acetate were added and the reaction mixture was stirred at 25 °C for 5h. To get 5-chloro-*N*-phenylbenzo[*d*]oxazol-2-amine derivatives (**13**) with 80-90% yield (**Figure 2**).[86]

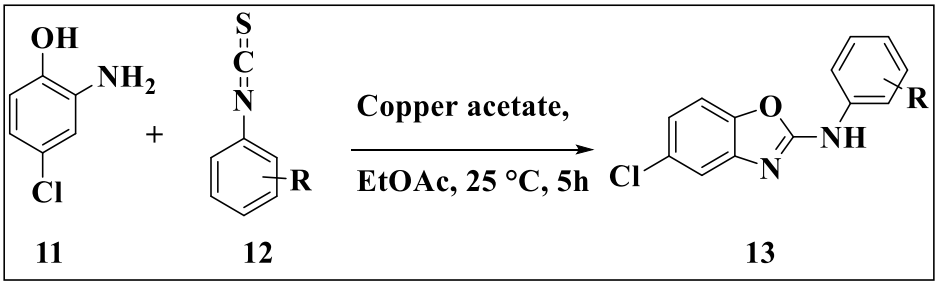


**Figure 2**

But-3-en-2-one (**15**) and 1,8-diazabicyclo[5.4.0]undec-7ene (DBU) were added to a solution to tert-butyl (2((5-chlorobenzo[*d*]oxazole-2-yl)amino)ethyl)carbamate derivatives (**14**) in DMF at 0-5 °C, and reaction was stirred at 25 °C for 16h. To get tert-butyl (2-((5-chlorobenzo[*d*]oxazol-2-yl)(3-oxobutyl)amino)ethyl)carbamate darivatives (**16**) (**Figure 3**).[87]

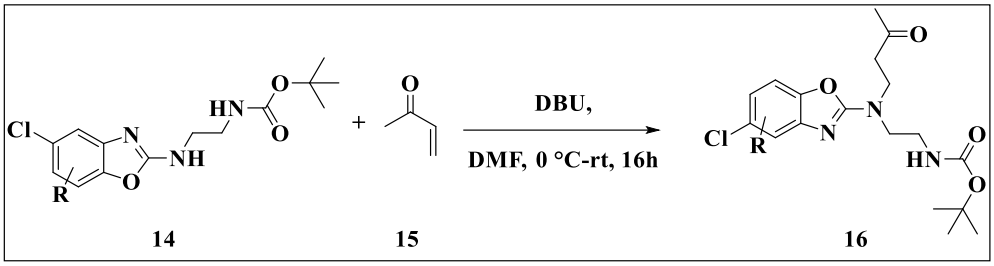


**Figure 3**

To a mixture of o-substituted anilines derivatives (**11**) and 1,3-diketones (**17**) in THF was added 30% w/w aqueous $NaICl_2$, and reaction was stirred at 70 °C for 2h. To get derivatized 5-chloro-2-methylbenzo[*d*]oxazole (**18**) (**Figure 4**).[88]

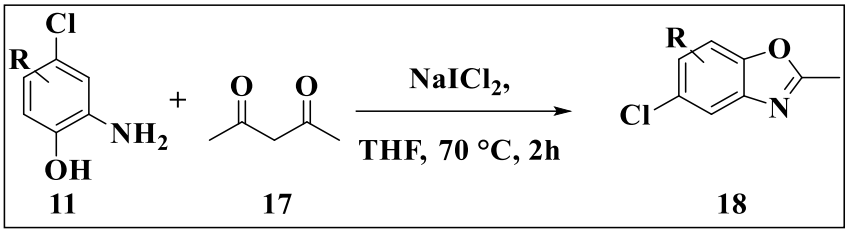


**Figure 4**

A mixture of some 2-amino-4-chlorophenol derivatives (**11**), potassium hydroxide, and carbon disulphide in ethanol and water and stirred at 80 °C for 3h to get derivatized 5-chlorobenzo[*d*]oxazole-2-thiol (**19**) (**Figure 5**).[89]

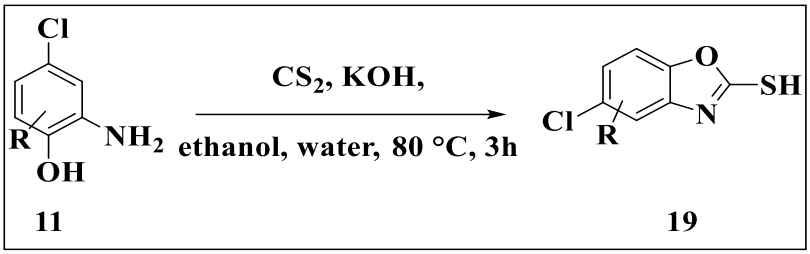


**Figure 5**

Compound 5-chlorobenzo[*d*]oxazole-2-thiol (**19**), 2-bromo-2-fluoro-1-phenylethan-1-one (**20**) and $K_2CO_3$ stirred in THF. The reaction was stirred for 25 °C for 2h for generate the 2-((5-chlorobenzo[*d*]oxazol-2-yl)thio)-2-fluoro-1-phenylethan-1-one (**21**) (**Figure 6**).[90]

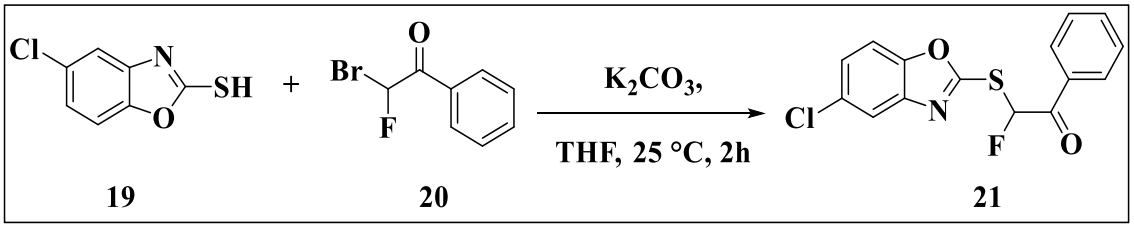


**Figure 6**

For the preparation of the derivatives 5-chlorobenzo[*d*]oxazol-2-amine (**23**) via cyclisation of derivatives 2-amino-4-chlorophenol (**11**) in methanol, cyanogen bromide (**22**) was added at 0°C in a dropwise and reaction was stirred at 25 °C for 16h (**Figure 7**).[91]

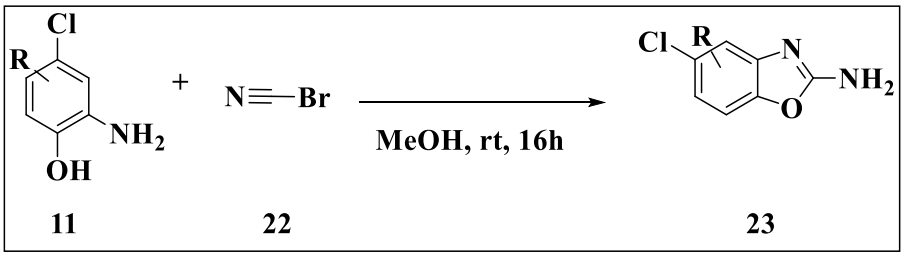


**Figure 7**

S-((5-chlorobenzo[*d*]oxazol-2-yl)methyl)ethanethioate (**24**) by using methanol:water (5:1) and $K_2CO_3$ and reaction was stirred at 25 °C for 2 h to generate the (5-chlorobenzo[*d*]oxazol-2-yl)methanethiol (**25**) (**Figure 8**).[92]

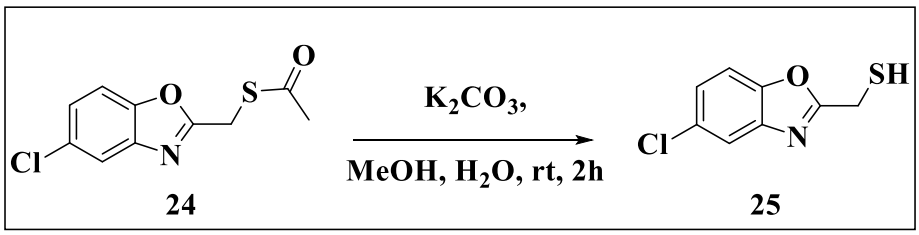


**Figure 8**

Some important benzoxazole derivatives having biological activity, such as anticancer (**26**),[93] antitubercular (**27**),[94] antibacterial (**28**),[95] antiprotozole (**29**),[96] anthelmintic (**30**),[97] antiinflamatory (**31**),[98] and antibiotic (**32**)[99] (**Figure 9**).

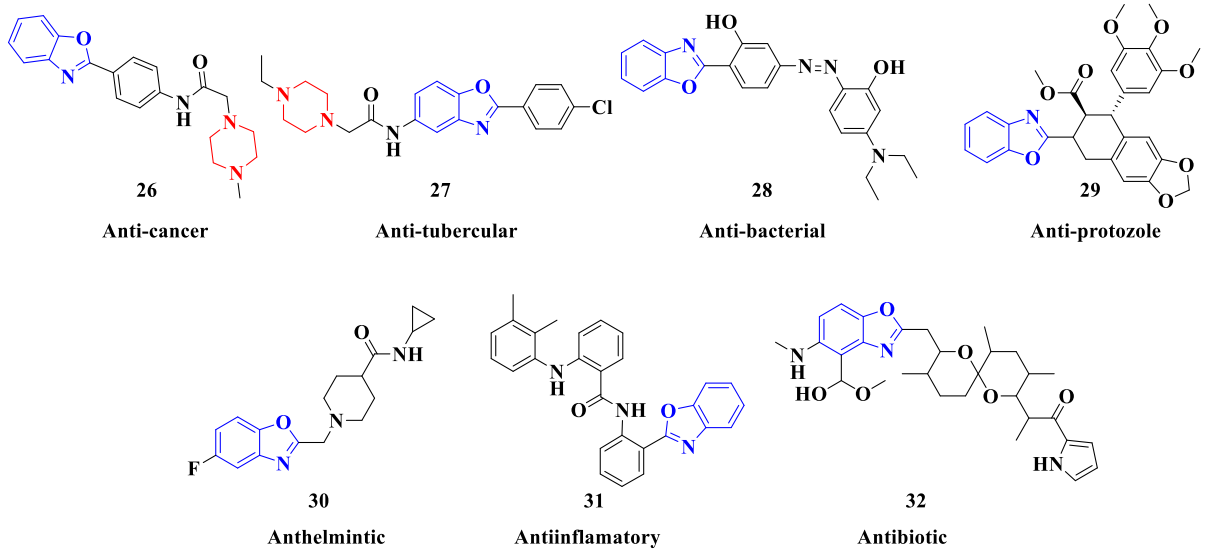


**Figure 9:** Important compounds containing Benzoxazole and piperazine motifs.

## 2.2 Results and Discussion

### 2.2.1 Chemistry

In order to investigate the various chemical and possible pharmacological characteristics of benzoxazole-piperazine hybrids with amide linkages (**9a-n**), a carefully designed series of procedures focused at functional group modification was used to create the final compounds (Scheme 1). Following a reported procedure, the process started with the amide formation of 2-amino-4-chlorophenol (**1**), which reacted with ethyl 2-chloro-2-oxoacetate (**2**) to yield ethyl 2-((5-chloro-2-hydroxyphenyl)amino)-2-oxoacetate (**3**) in 77% yield.[100] This was confirmed by figureits $^{1}$H NMR data, which showed an amide proton singlet at δ 10.65 ppm and a phenol (OH) singlet at δ 9.65 ppm, both of which were exchangeable in $D_2O$. Under Mitsunobu conditions, compound **3** underwent intramolecular cyclization, yielding 81% ethyl 5-chlorobenzo[*d*]oxazole-2-carboxylate (**4**).[101] Compound **4** was then reacted with 1-boc piperazine (**5**) via ester-amine coupling using trimethylaluminium (TMA, 2M in toluene) at 110 °C, yielding *tert-butyl* 4-(5-chlorobenzo[*d*]oxazole-2-carbonyl)piperazine-1-carboxylate (**6**) with a 54% yield and 97% purity as determined by LC-MS analysis.[102] The *N*-Boc deprotection of compound **6** was performed using 4M HCl in dioxane, resulting in (5-chlorobenzo[*d*]oxazol-2-yl)(piperazin-1-yl)methanone hydrochloride (**7**) with a 90% yield.[103] The final compounds (**9a-n**) were synthesized through acid-amine coupling of compound **7** with substituted benzoic acids (**8a-n**) utilizing HATU and DIPEA in DMF as a solvent.[104] The synthesized compounds were isolated with purity exceeding 95% as confirmed by LC-MS, elemental analysis, $^{1}$H NMR, $^{13}$C NMR, and FTIR spectroscopy.

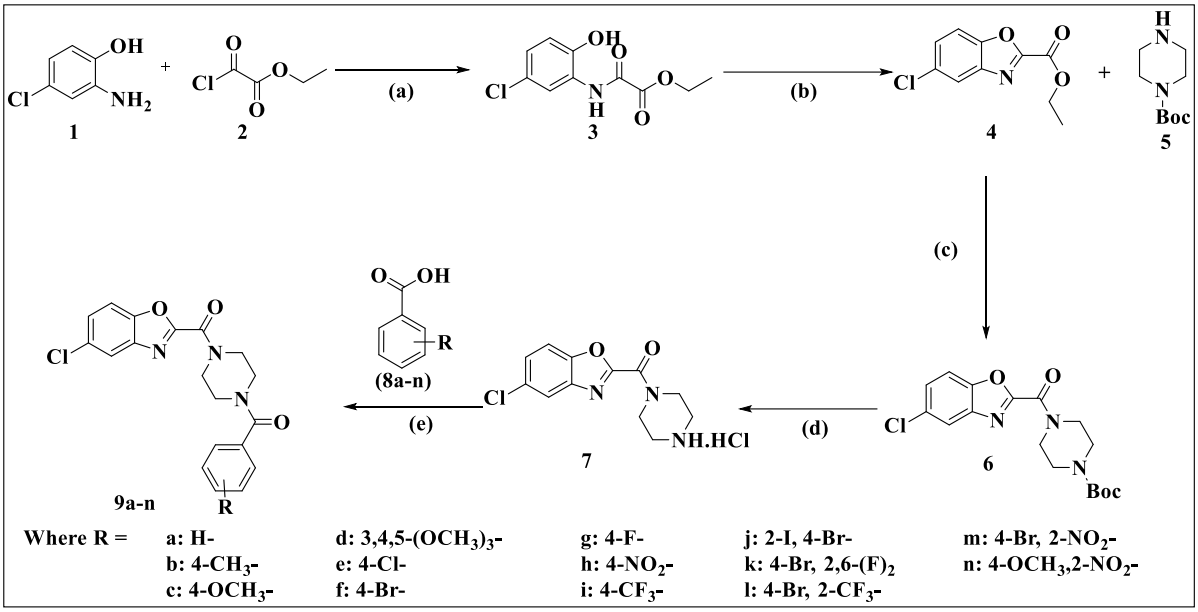


**Reaction conditions:** a) TEA (2 eq), DMF, 0 °C, rt, 3h; b) triphenylphosphine (1.5 eq), DIAD (1.5 eq), THF, 0 °C, rt, 3h; c) TMA (1.5 eq), toluene, 110 °C, 16h; d) 4M HCl in dioxane, ethyl acetate rt, 16h; e) HATU (1.5 eq), DIPEA (3 eq), DMF, 0 °C, rt, 16h.

**Scheme 1:** Synthesis of benzoxazole-piperazine hybrid with amide linkage (**9a-n**).

**Table 1:** Physicochemical characteristics of the novel benzoxazole-piperazine derivatives **9a-n**.

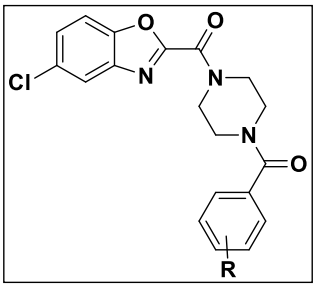

| Comp. | R | Molecular Weight | Molecular Formula | Yield (%) | Melting Point (°C) |
|---|---|---|---|---|---|
| **9a** | H | 369.80 | $C_{19}H_{16}ClN_3O_3$ | 82 | 172-175 |
| **9b** | 4-Me | 383.83 | $C_{20}H_{18}ClN_3O_3$ | 78 | 135-138 |
| **9c** | 4-OMe | 399.83 | $C_{20}H_{18}ClN_3O_4$ | 83 | 127-130 |
| **9d** | 3,4,5-OMe | 459.88 | $C_{22}H_{22}ClN_3O_6$ | 83 | 127-130 |
| **9e** | 4-Cl | 404.25 | $C_{19}H_{15}Cl_2N_3O_3$ | 89 | 169-170 |
| **9f** | 4-Br | 448.70 | $C_{19}H_{15}BrClN_3O_3$ | 85 | 172-175 |
| **9g** | 4-F | 387.79 | $C_{19}H_{15}ClFN_3O_3$ | 90 | 199-202 |

| | | | | | |
|---|---|---|---|---|---|
| **9h** | 4-$NO_2$ | 414.80 | $C_{19}H_{15}ClN_4O_5$ | 88 | 230-233 |
| **9i** | 4-$CF_3$ | 437.80 | $C_{20}H_{15}ClF_3N_3O_3$ | 78 | 167-171 |
| **9j** | 2-I, 4-Br | 574.59 | $C_{19}H_{14}BrClIN_3O_3$ | 71 | 187-191 |
| **9k** | 4-Br,2,6-F | 484.68 | $C_{19}H_{13}BrClF_2N_3O_3$ | 73 | 160-164 |
| **9l** | 4-Br, 2$CF_3$ | 516.70 | $C_{20}H_{14}BrClF_3N_3O_3$ | 83 | 129-132 |
| **9m** | 4-Br, 2-$NO_2$ | 493.70 | $C_{19}H_{14}BrClN_4O_5$ | 94 | 147-150 |
| **9n** | 4-$OCH_3$, 2-$NO_2$ | 444.83 | $C_{20}H_{17}ClN_4O_6$ | 95 | 197-200 |

## 2.3 Antimicrobial Activity

The nutrient agar disk diffusion technique was used to assess the antibacterial activity of the recently synthesized hybrid benzoxazole-piperazine derivatives with substituted amides (**9a-n**). Gram-positive bacteria (*B. subtilis* ATCC6051 and *S. aureus* ATCC12600), gram-negative bacteria (*P. aeruginosa* ATCC10415 and *E. coli* ATCC9637), and fungal strains (*A. niger* (ATCC 16888) and *C. albicans* (ATCC 10231)) were used to assess the synthetic compounds activity. The negative control was DMSO, while the positive controls for antibacterial and antifungal activities were chloramphenicol (30 µg/disc) and gentamicin (10 µg/disc) and nystatin, respectively. The zones of inhibition for each produced drug against the four bacterial strains and two fungal strains (**Figures 10 and 11**) in comparison to the reference standards gentamicin and chloramphenicol. Using the disc diffusion technique, the test was conducted on nutritional agar containing sodium chloride (5.0 g/L), yeast extract (10.0 g/L), and peptone (10.0 g/L) at a pH of 7.2.[105] Compound **9f** had the strongest antibacterial activity among the compounds tested against every bacterial species examined.

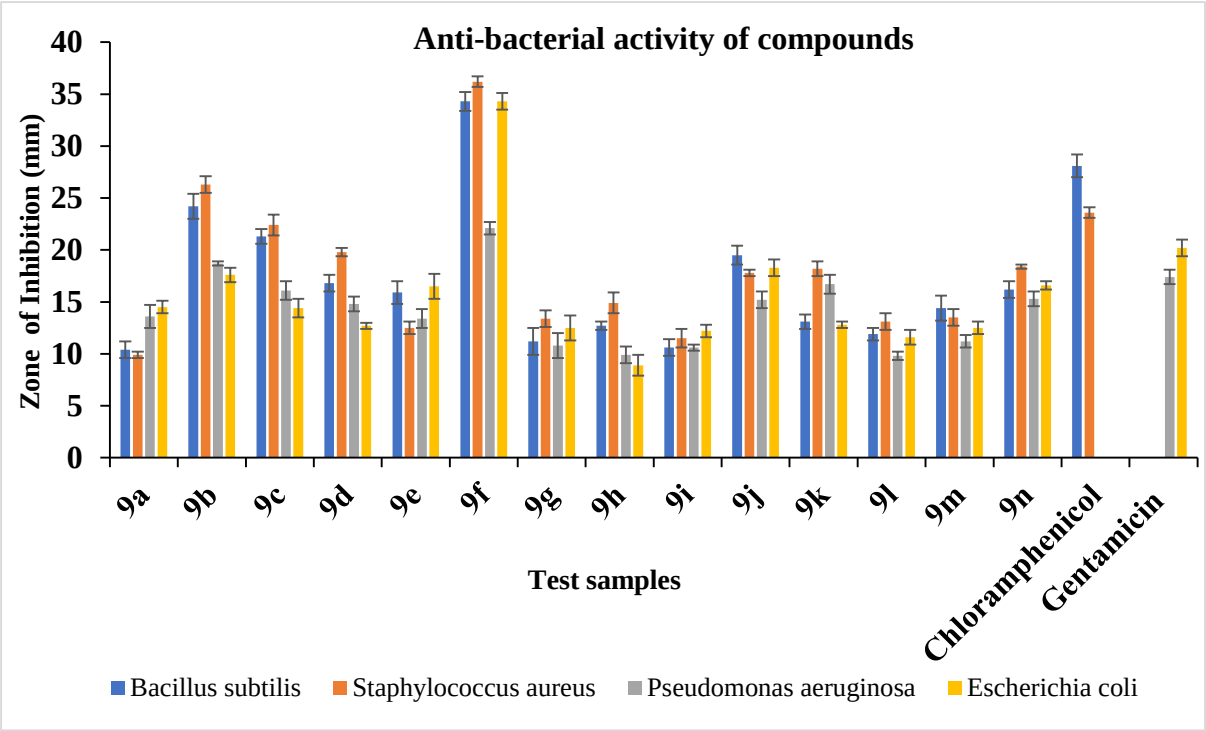


**Figure 10:** Graphical presentation of anti-bacterial activity data of newly synthesized benzoxazole-piperazine hybrid with amide linkage **9a-n**.

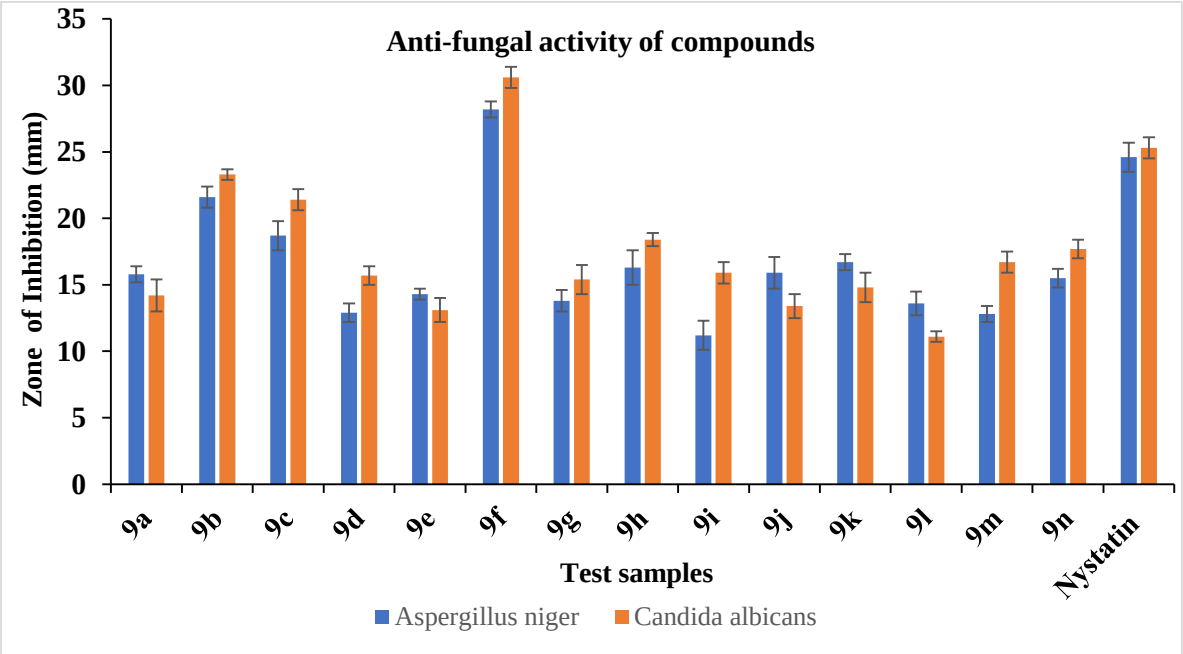


**Figure 11:** Graphical presentation of anti-fungal activity data of newly synthesized benzoxazole-piperazine hybrid with amide linkage **9a-n**.

## 2.4 Structure Activity Relationship (SAR)

*B. subtilis* (34.3 ± 0.9 mm) and *S. aureus* (36.2 ± 0.5 mm) were two gram-positive pathogens that compound **9f**, which has a para-position (4-Br) substitution, shown moderate to strong antibacterial activity. In contrast, the conventional medication chloramphenicol showed inhibition zones against the corresponding infections of 28.1 ± 1.1 mm and 23.6 ± 0.5 mm. Against gram-negative pathogens, compound **9f** demonstrated noteworthy antibacterial activity, with inhibition zones of 22.1 ± 0.6 mm for *E. coli* and 34.3 ± 0.8 mm for *P. aeruginosa*. Conversely, smaller inhibition zones of 17.4 ± 0.7 mm and 20.2 ± 0.8 mm were shown by the common medication gentamicin. In contrast to compound **9f**, compound **9j**, which has both an ortho-position (I) and a para-position (Br) substitution, showed less antibacterial efficacy against gram-positive and gram-negative microorganisms. In addition, out of all the compounds examined, compound **9a** with no modification (H) showed the least amount of antibacterial activity against both kinds of infections.

Furthermore, compound **9f** exhibited moderate to high antifungal activity against *A. niger* (28.2 ± 0.6 mm) and *C. albicans* (30.6 ± 0.8 mm), whereas the usual medication nystatin showed activity against the same pathogens of 24.6 ± 1.1 mm and 25.3 ± 0.5 mm, respectively. Comparing compound **9j** to compound **9f**, the former showed less antifungal efficacy against *A. niger* and *C. albicans*. Compound **9i**, which has a replacement for $CF_3$, on the other hand, showed the least amount of antifungal efficacy against both fungal strains after testing.

## 2.5 Molecular Docking

The molecular docking investigation gave important information about the chemicals' stability and possible strength of interaction inside the protein binding pocket.[106] With the highest negative binding affinity of -7.8 kcal/mol among the compounds examined, **9f** was the most promising candidate (Table 2). Its great affinity is consistent with its interaction profile's strong hydrogen bonding, ideal interaction distances, and notable hydrophobic interactions. The substantial binding affinities of **9b** (-7.7 kcal/mol) and **9c** (-7.5 kcal/mol) further highlighted their reliable and efficient interactions with the protein target. These compounds' durability and strong antibacterial activity are probably attributed to the many hydrogen bonds they establish with important residues while preserving advantageous hydrophobic interactions. Although it was somewhat

less efficient than compounds **9f** and **9b**, compound **9n** (-7.5 kcal/mol) showed a binding affinity similar to that of **9c**, indicating that it is another promising candidate for antibacterial action. Chemicals **9j** (-7.3 kcal/mol) and **9l** (-7.4 kcal/mol), on the other hand, had modest binding affinities. In contrast, the compounds with the least favorable binding affinities, **9d** (-6.6 kcal/mol), **9e** (-6.7 kcal/mol), and **9g** (-6.7 kcal/mol) showed poorer interaction patterns. These substances probably have fewer hydrophobic and hydrogen bonding interactions or have less-than-ideal interaction geometries, which lowers their stability and binding effectiveness inside the protein pocket.

To assess their potential for antimicrobial activity, the protein-ligand interactions for lead compounds **9b**, **9c**, and **9f** were examined (**Figures 12, 13, and 14**); similarly, the interactions for chloramphenicol were examined to assess their potential for antimicrobial activity (**Figure 15**). In order to determine binding stability and efficacy, the evaluation concentrated on the types and strengths of interactions, such as ionic, hydrophobic, and hydrogen bonding interactions. Compound **9b** stabilizes itself inside the binding pocket by forming hydrogen bonds with important residues, including ARG (3.23 Å) and THR (3.13 Å). Stability is further improved by hydrophobic interactions with residues such as LYS and PRO. Nevertheless, certain interactions (like 5.10 Å) take place near the upper end of the permissible distance range, suggesting perhaps less-than-ideal binding. Compound **9c** contributes to stable binding by forming hydrogen bonds with residues like ARG (3.20 Å) and GLU (3.14 Å). However, some interaction distances, like 5.39 Å, are outside of the ideal range, indicating that the compound is not as well anchored in the pocket. However, compound **9f** provides strong anchoring at the binding site by forming strong hydrogen bonds with important residues such as ARG (3.22 Å) and THR (3.19 Å). Furthermore, the binding is further stabilized by strong hydrophobic interactions with residues like PRO and LYS.

**Table 2:** Molecular docking results of the newly synthesized compounds (**9a-n**) against *E. coli* DNA gyrase B protein receptor (PDB: 4DUH).

| **Comp.** | **Binding affinity (kcal/mol)** | **Interacting residues (A°)** | **No. of H-Bonds** |
|---|---|---|---|
| **9a** | -7.4 | Asp17 (3.51), Arg20 (4.44), Arg20 (2.94), Thr175 (2.72), Arg204 (2.96), Thr30 (3.19) | 04 |

| | | | |
|---|---|---|---|
| **9b** | -7.7 | Lys24 (4.67) Lys24 (4.04), Arg204 (3.23), Pro23 (5.39) Pro23(4.18), Thr175 (3.13), Arg20 (5.10) Arg20 (3.55) | 03 |
| **9c** | -7.5 | Lys10 (4.10), Lys10 (4.60), Arg204 (3.20), Pro23 (4.14), Pro23 (5.39), Thr175 (3.14), Arg20 (5.08), Arg20 (3.54) | 02 |
| **9d** | -6.6 | Gly75 (2.06), Ile94 (2.21), Gly101 (2.12), Glu50 (2.11), Gly102 (2.16), Thr 165 (2.83), Gly 77 (2.81) | 03 |
| **9e** | -6.7 | Arg204 (3.23), Arg204 (3.03), Arg20 (3.44), Thr175 (3.58) | 03 |
| **9f** | -7.8 | Lys21 (4.74), Lys21 (4.20), Arg204 (3.22), Pro23 (4.21), Pro23 (5.40), Thr175 (3.12), Arg20 (5.09), Arg20 (3.51) | 02 |
| **9g** | -6.7 | Arg204 (3.23), Arg20 (3.05), Arg20 (3.59), Thr175 (3.38) | 03 |
| **9h** | -6.9 | Ala100 (3.20), Phe104 (3.52), Gly103 (3.93), Gly117 (3.47) | 03 |
| **9i** | -7.5 | Gly101 (2.83), Asn46 (3.20), Ala100 (3.20), Gly81 (3.33), Gly117 (3.34), Asp34 (3.34), Val44 (4.96), Ile94 (5.10), Ile78 (5.44), Ile113 (5.44), Val120 (4.96), Asn45 (3.78), Asp83 (3.83) | 02 |
| **9j** | -7.3 | Thr175 (2.98), Thr175 (2.93), Arg20 (3.76) Lys21 (4.15), Pro23 (5.12), Pro23 (5.31), Arg20 (4.90) | 03 |
| **9k** | -7.0 | Arg204 (2.24), Thr175 (3.00), Arg 20 (4.46), Thr30 (3.21) Asp17 (2.10), Asp17 (3.38) Lys21 (4.58), Pro23 (5.40), Pro23 (4.18) | 03 |
| **9l** | -7.4 | Thr175 (3.07), Thr175 (3.01), Thr175 (3.81), Lys21 (4.27), Arg20 (4.75), Arg20 (3.56), Pro23 (5.31), Pro23 (5.17) | 03 |
| **9m** | -6.9 | Thr175 (2.84), Lys21 (2.84), Arg204 (2.29), Arg20 (4.95), Arg20 (3.96), Arg204 (4.59), Pro23 (4.24), Arg22 (4.44), Arg22 (3.74), Pro23 (5.39) | 03 |
| **9n** | -7.5 | Arg204 (2.44), Arg204 (2.94), Arg20 (2.97), Thr175 (3.54), Pro23 (5.40), Pro23 (4.19), Lys21 (4.06), Lys21 (4.64), Ser202 (3.46), Asp17 (3.36), Arg20 (4.22) | 04 |
| **Chloramphenicol** | -6.8 | Gly101 (2.16), Glu50 (3.96), Ile78 (4.92), Pro79 (5.45), Lys103 (4.14), Arg76 (3.20), Gly77 (2.80), Thr165 (2.86) | 04 |

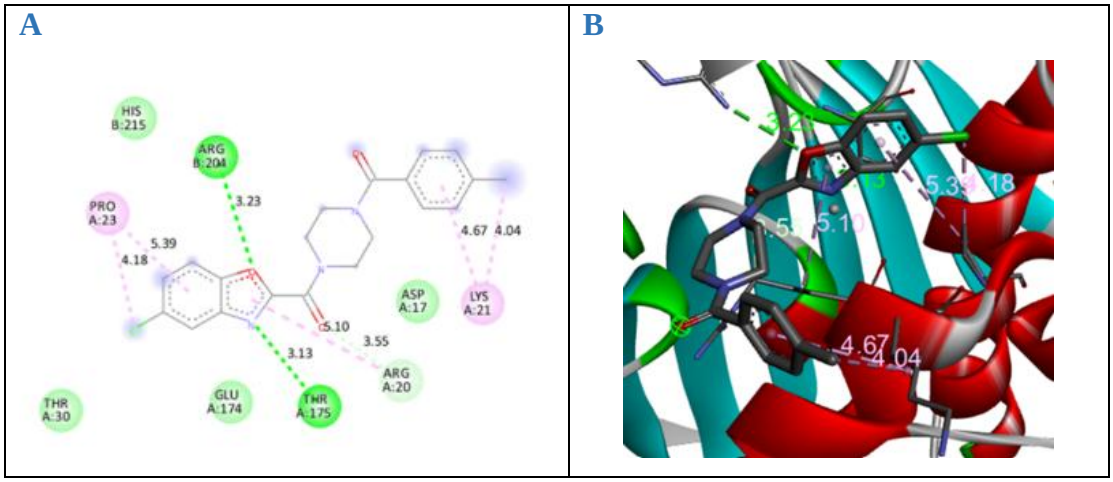


**Figure 12:** Docking pose of compound **9b** with 24 kDa domain of *E. coli* DNA gyrase. (**A**) Receptor-ligand interaction on a 2D diagram, (**B**) Receptor-ligand interaction on a 3D diagram.

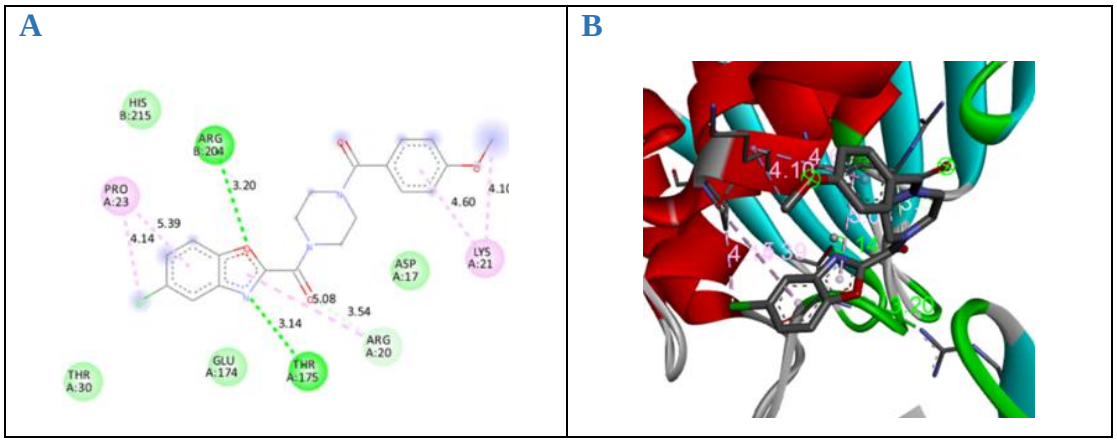


**Figure 13:** Docking pose of compound **9c** with 24 kDa domain of *E. coli* DNA gyrase. (**A**) Receptor-ligand interaction on a 2D diagram, (**B**) Receptor-ligand interaction on a 3D diagram.

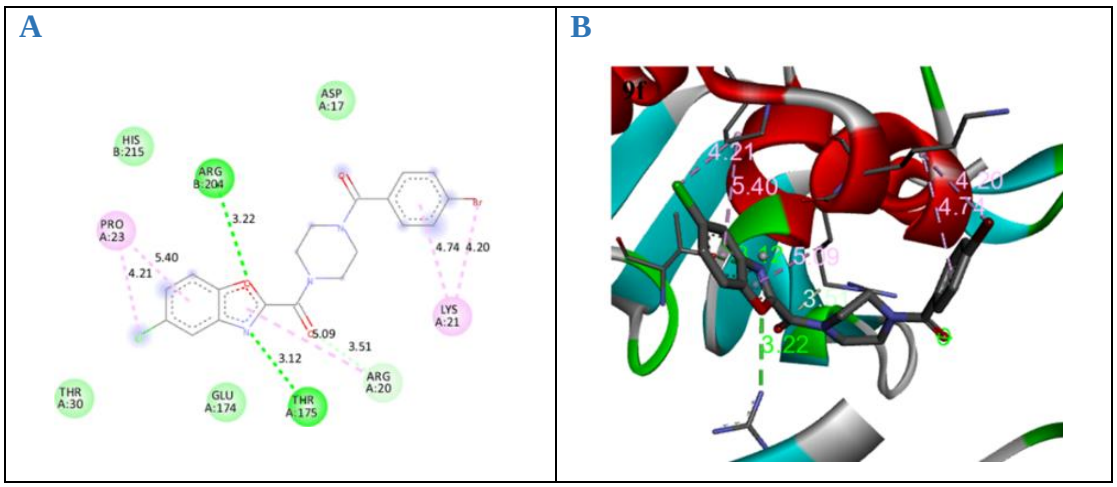


**Figure 14:** Docking pose of compound **9f** with 24 kDa domain of *E. coli* DNA gyrase. (**A**) Receptor-ligand interaction on a 2D diagram, (**B**) Receptor-ligand interaction on a 3D diagram.

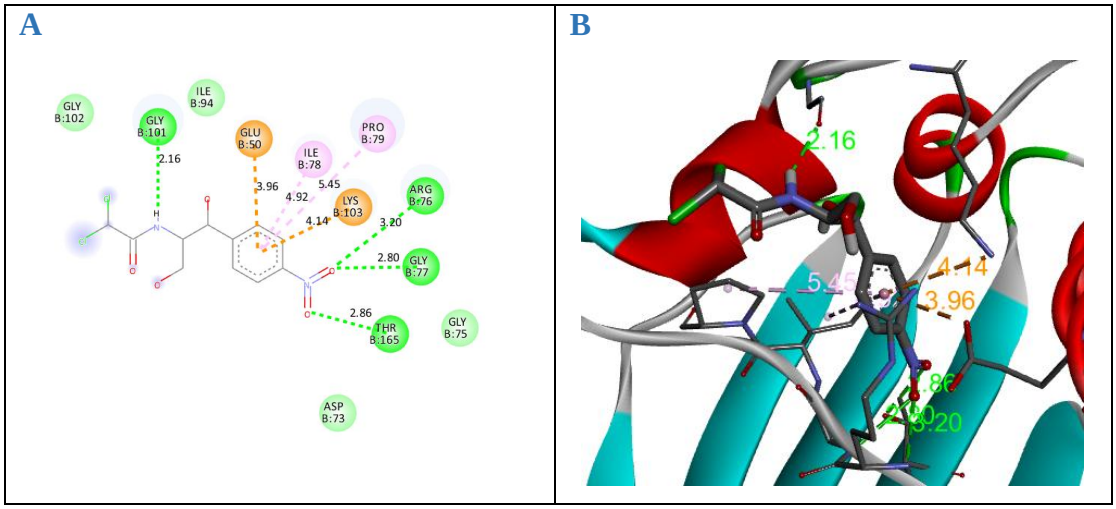


**Figure 15:** Docking pose of chloramphenicol with 24 kDa domain of *E. coli* DNA gyrase. (**A**) Receptor-ligand interaction on a 2D diagram, (**B**) Receptor-ligand interaction on a 3D diagram.

## 2.6 Molecular Dynamics Simulation Analysis

Compound **9f** was chosen for further examination by molecular dynamics simulation (MDS) based on the docking analysis. In MDS, the root mean square deviation (RMSD) and root mean square fluctuation (RMSF) offer complementary insights into the structural dynamics of the protein-ligand complex during the simulation duration.[107] The RMSD graph for compound **9f** illustrates the overall stability of both the protein and the ligand during the simulation (**Figure 16**). The protein RMSD stabilizes between 1.25 and 1.75 Å after the first 10 to 15 nanoseconds, signifying that the protein reached equilibrium and sustained a stable shape throughout the 100-nanosecond simulation. The ligand RMSD remained consistently low, oscillating between 1.0 and 2.5 Å, indicating that the ligand was securely attached inside the protein's binding pocket, without notable displacement or detachment. The lack of significant fluctuations in both the protein and ligand RMSD further confirmed the stability and dependability of the simulation.

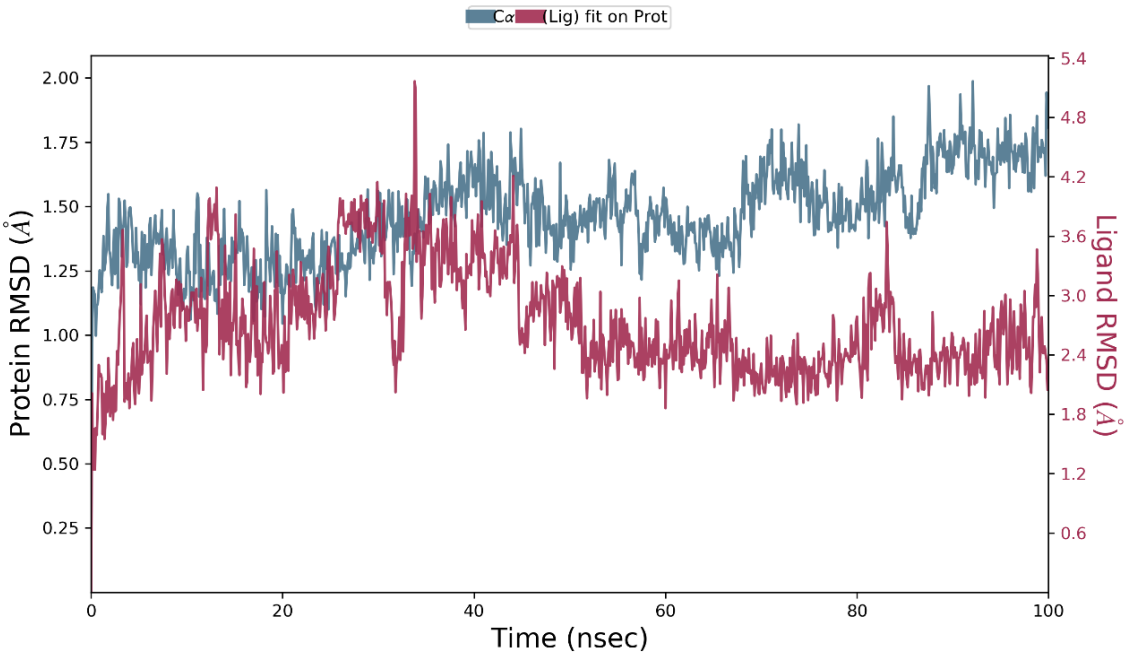


**Figure 16:** RMSD plot of compound **9f**-4DUH complex.

Conversely, the RMSF offered residue-specific insights regarding the protein's flexibility during the simulation.[108] The peaks on the RMSF graph indicate areas of increased flexibility, including terminal residues and loop regions, whereas other areas exhibited relative stability (**Figure 17**). The results validate that compound **9f** establishes a stable combination with the protein, positioning it as a robust contender for further advancement in antimicrobial applications. These regions generally display greater variability as they lack the constraints of secondary structural elements like alpha-helices or beta-sheets. Conversely, the central residues and secondary structural components have reduced RMSF values, often beneath 1.5 Å, signifying their stiffness and structural stability. Several residues near the midpoint and adjacent to the C-terminal exhibit moderate flexibility, with RMSF values nearing 3 Å. These probably relate to loop areas or dynamic domains. The interaction fraction graph emphasizes key residues, such as ARG_136, ARG_76, ASP_73, and LYS_103, which establish important hydrogen bonds and hydrophobic interactions. These acids are crucial for maintaining the protein-ligand complex and demonstrate persistent interactions during the simulation, confirming robust ligand binding (**Figure 18**).

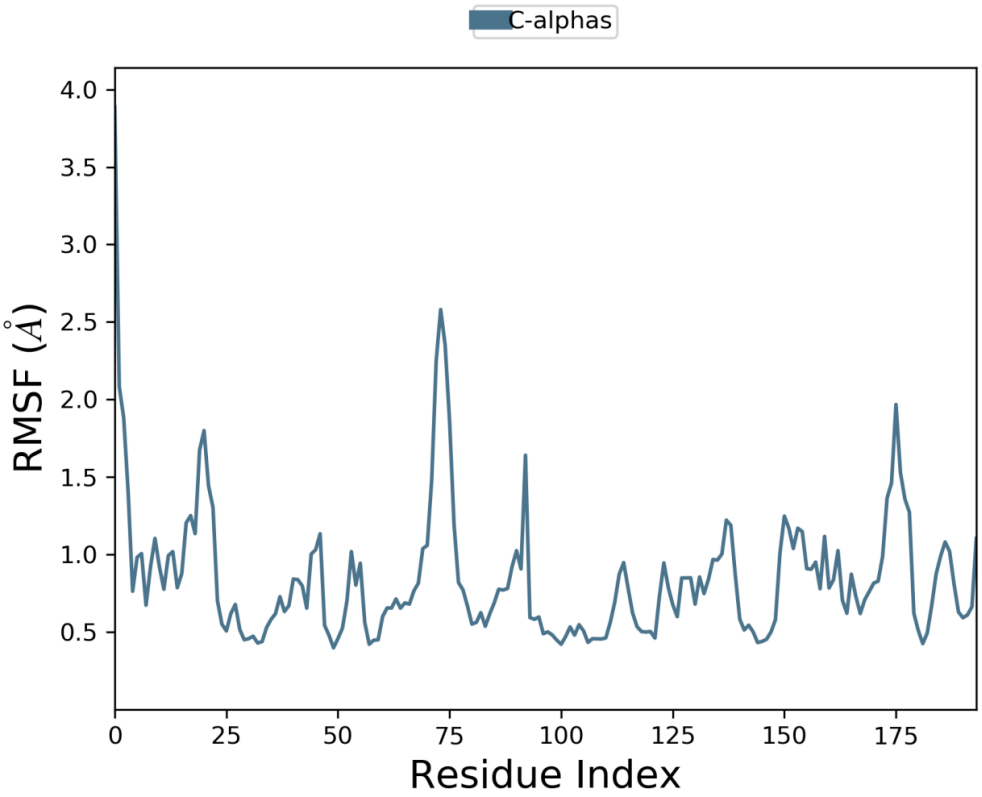


**Figure 17:** RMSF plot of compound **9f**-4DUH complex.

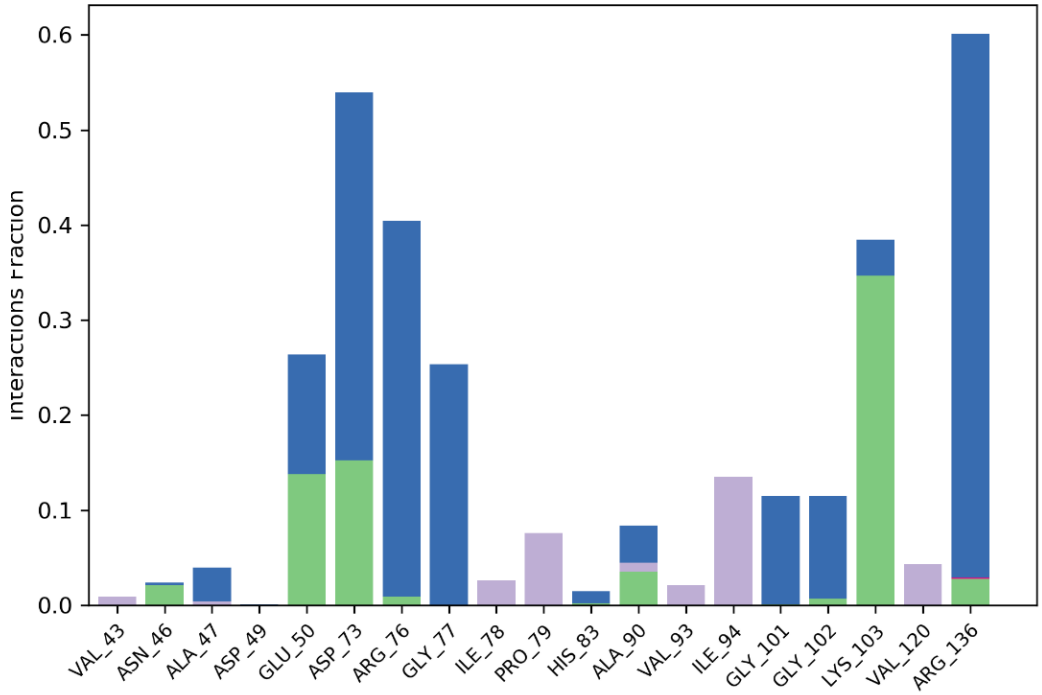


**Figure 18:** Interaction graph of compound **9f**-4DUH contacts.

## 2.7 ADMET evaluation

A multitude of prospective drug candidates do not advance in the drug development process owing to insufficient pharmacokinetic and physicochemical characteristics.[109] Utilizing SwissADMET methodologies to assess freshly synthesized compounds enables the early identification and rectification of these deficiencies in the first stages of research.[110] The evaluation of the ADMET characteristics of the newly synthesized benzoxazole hybrid compounds, as shown in Table 3, indicated that the water solubility (Log S) values varied from -4.25 to -6.95, suggesting their potential bioavailability. The lipophilicity (Log Po/w) values were determined to be below 5, namely between 1.94 to 4.31, indicating advantageous membrane permeability. All produced compounds conformed to Lipinski's rule of five, except for compounds **9k** and **9l**, which possessed molecular weights more than 500. Moreover, all the benzoxazole hybrid compounds had lipophilicity scores between 1.94 and 4.31, underscoring their potential for drug-like characteristics.

**Table 3:** ADMET properties of newly synthesized benzoxazole-piperazine hybrid with amide linkage **9a-n**.

| Comp. | Physicochemical properties | | | | | | Pharmacokinetics | | Medicinal chemistry | |
|---|---|---|---|---|---|---|---|---|---|---|
| | M.W.[#] | HBA | HBD | TPSA | Log Po/w | Log S | GIA | Log kp | ROF | SA |
| **9a** | 369.80 | 4 | 0 | 66.65 | 2.69 | -4.25 | High | -6.35 | 0 | 2.87 |
| **9b** | 383.83 | 4 | 0 | 66.65 | 3.06 | -4.56 | High | -6.17 | 0 | 2.99 |
| **9c** | 399.83 | 5 | 0 | 75.88 | 2.73 | -4.33 | High | -6.55 | 0 | 2.96 |
| **9d** | 459.88 | 7 | 0 | 94.34 | 2.69 | -4.49 | High | -6.95 | 0 | 3.35 |
| **9e** | 404.25 | 4 | 0 | 66.65 | 3.25 | -4.85 | High | -6.11 | 0 | 2.88 |
| **9f** | 448.70 | 4 | 0 | 66.65 | 3.33 | -5.17 | High | -6.33 | 0 | 2.90 |
| **9g** | 387.80 | 5 | 0 | 66.65 | 3.02 | -4.41 | High | -6.39 | 0 | 2.89 |
| **9h** | 414.80 | 6 | 0 | 112.47 | 1.97 | -3.93 | High | -6.74 | 0 | 3.04 |
| **9i** | 437.80 | 7 | 0 | 66.65 | 3.71 | -5.11 | High | -6.13 | 0 | 3.00 |
| **9j** | 574.60 | 4 | 0 | 66.65 | 3.97 | -6.34 | High | -6.64 | 1 | 3.05 |
| **9k** | 484.68 | 6 | 0 | 66.65 | 3.92 | -5.49 | High | -6.41 | 0 | 2.96 |
| **9l** | 516.70 | 7 | 0 | 66.65 | 4.31 | -6.03 | High | -6.12 | 1 | 3.09 |
| **9m** | 493.70 | 6 | 0 | 112.47 | 2.59 | -5.23 | High | -6.73 | 0 | 3.22 |

| | | | | | | | | | | |
|---|---|---|---|---|---|---|---|---|---|---|
| **9n** | 444.83 | 7 | 0 | 121.7 | 1.94 | -4.39 | High | -6.95 | 0 | 3.32 |
| **Doxycycline** | 444.43 | 9 | 6 | 181.62 | -0.50 | -2.35 | Low | -8.63 | 0 | 5.25 |
| #Hydrogen Bond Acceptors (HBA), Hydrogen Bond Donors (HBD), Topological Polar Surface Area (TPSA), Lipophilicity (Log Po/w), Water Solubility (Log S), Gastrointestinal Absorption (GIA), Skin permeation (Log Kp), Lipinski's rule of five (RoF) and Synthetic Accessibility (SA). | | | | | | | | | | |

## 2.8 Experimental Section

### 2.8.1 Chemistry

**Synthesis of {Ethyl 2-[(5-chloro-2-hydroxyphenyl)amino]-2-oxoacetate} (3)**

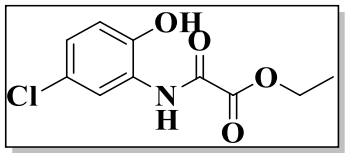


Compound {Ethyl 2-[(5-chloro-2-hydroxyphenyl)amino]-2-oxoacetate**}** **(3)** was synthesized using a previously reported method with yield: 77%. mp: 125-127 °C (Reported mp: 125-128 °C).[100]

**Synthesis of ethyl 5-chlorobenzo[*d*]oxazole-2-carboxylate (4)**

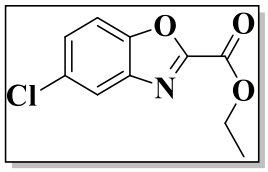


TPP (32.34 g, 0.123 mol) and DIAD (24.98 g, 0.123 mol) were added to a solution of {Ethyl 2-[(5-chloro-2-hydroxyphenyl)amino]-2-oxoacetate} (**3**) (20 g, 0.082 mol) in THF (200 mL) in 3-neck RBF at 0 °C under a nitrogen environment. For three hours, the reaction was agitated at room temperature. Using the proper mobile phase and TLC, the product's formation and the starting material's consumption were tracked. After the reaction was finished, it was quenched with water and extracted twice or three times using ethyl acetate. To obtain the crude product, the mixed organic layer was dried over sodium sulfate, filtered, and the solvent was evaporated until it was completely dry. Column chromatography employing 60–120 silica gel was used to purify the crude product, which was then eluted using 0–20% ethyl acetate in hexane. Ethyl (5-chlorobenzo[*d*]oxazol-2-yl)carboxylate (**4**), off white (15 g, 81% yield).[101] mp: 135-138 °C. Off-white solid. IR (KBr) νmax/cm$^{-1}$: 3084 (aromatic-CH), 2912 (aliphatic-CH), 1725 (COO), 1638 (C=N), 1545 (C=O). $^{1}$H NMR (400 MHz, *DMSO-d*$_6$): δppm

8.09-8.08 (d, J=2Hz, 1H, Ar-CH), 7.97-7.94 (d, J = 8.8 Hz, 1H, Ar-CH), 7.67-7.65 (q, J = 6.5Hz, 1H, Ar-CH), 4.46-4.41 (q, J = 7.2Hz, 2H, CH2), 1.38-1.34 (t, J = 6.8Hz, 3H, CH3). $^{13}$C NMR (100 MHz, *DMSO-d*$_6$): 155.98, 154.41, 149.41, 141.65, 130.44, 128.83, 121.70, 113.95, 63.26, 14.33. LC-MS (*m/z*): 97%, $[M]^+$ : 226, $[M+1]^+$ : 227. Anal. Calcd. $C_{10}H_8ClNO_3$ (225.63): C, 53.23; H, 3.57; N, 6.21%. Found C, 53.35; H, 3.49; N, 6.26%.

**Procedure for synthesis of *tert-butyl* 4-(5-chlorobenzo[*d*]oxazole-2-carbonyl)piperazine-1-carboxylate (6)**

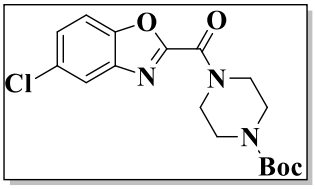


At 0 °C, trimethyl aluminum (TMA, 2M in toluene) (63 mL, 7.20 g, 0.099 mol) was added to a solution of tert-butyl piperazine-1-carboxylate (**5**, 18.57 g, 0.099 mol) in toluene (150 mL) under a nitrogen environment. After 15 minutes of stirring, ethyl 5-chlorobenzo[*d*] oxazole-2-carboxylate (**4**, 15 g, 0.066 mol) was gradually added to the mixture. For 16h, the reaction was agitated at 110 °C, and TLC was used to track its development. After finishing, water was added and the liquid was allowed to cool to room temperature. Ethyl acetate was used three times to extract the mixture. To get the crude product, the mixed organic layer was cleaned with brine, dried on sodium sulfate, and then evaporated in a vacuum. Using 60–120 mesh silica gel, column chromatography was used to purify the crude product. 0–30% ethyl acetate in hexane was used to elute the product. Tert-butyl 4-(5-chlorobenzo[*d*]oxazole-2-carbonyl)piperazine-1-carboxylate (**6**), 16 g, 54% Yield.[102] mp: 154-157 °C. Off-white solid that was produced as the pure end product. IR (KBr) νmax/cm$^{-1}$: 2996 (aromatic-CH), 2916 (aliphatic-CH), 1682 (C=O), 1653 (C=O), 1537 (C=N), 1125 (C-N). 1H NMR (400MHz, *DMSO-d*$_6$): δppm 8.07 (s, 1H, Ar-CH), 7.94-7.92 (d, J = 8.4Hz, 1H, Ar-CH), 7.64-7.61 (q, J = 6.4Hz, 1H, Ar-CH), 3.95-3.93 (t, J = 4.8 Hz, 2H, CH2), 3.71-3.68 (t, J = 4.4 Hz, 2H, CH2), 3.46 (s, 4H, 2CH2), 1.43 (s, 9H, 3(CH3)). 13C NMR (100 MHz, *DMSO-d*$_6$): 150.04, 155.34, 153.70, 148.18, 140.77, 129.65, 127.44, 120.74, 113.08, 79.31, 46.21, 42.14, 28.01. LC-MS (m/z): 97%, $[M-56]^+$: 310, $[M-54]^+$: 312. Anal. Calcd. $C_{17}H_{20}ClN_3O_4$ (365.81): C, 55.82; H, 5.51; N, 11.49%. Found C, 55.78; H, 5.49; N, 11.53%.

**Procedure for synthesis of (5-chlorobenzo[*d*]oxazol-2-yl)(piperazin-1-yl)methanone hydrochloride (7)**

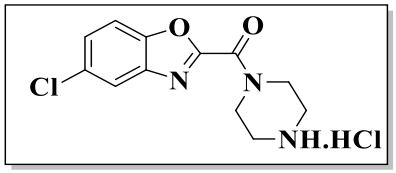


4M HCl in 50 mL of dioxane was added dropwise at 0 °C to agitate a solution of tert-butyl 4-(5-chlorobenzo[*d*]oxazole-2-carbonyl)piperazine-1-carboxylate (**6**, 16 g, 0.044 mol) in ethyl acetate (100 mL). After 16h of stirring the reaction mixture, TLC was used to track its development. After finishing, the solvent was removed using n-pentane and evaporated under low pressure, yielding the crude solid product (5-chlorobenzo[*d*]oxazol-2-yl)(piperazine-1-yl)methanone hydrochloride (**7**), off pink color (10.5 g, 90% yield).[103] mp : 110-112 °C. IR (KBr) νmax/cm$^{-1}$: 3367 (NH), 3071 (aromatic–CH), 2933 (aliphatic–CH), 1649 (C=O), 1587 (C-O), 1535 (C=N), 1138 (C-N). 1H NMR (400MHz, *DMSO-$d_6$*): 9.26 (s, 2H, (NH.HCl salt)), 8.06 (d, J = 2 Hz, 1H, Ar-CH), 7.95-7.93 (d, J = 8.8Hz, 1H, Ar-CH), 7.65-7.62 (m, 1H, Ar-CH), 4.28 (m, 2H, CH2), 3.92 (m, 2H, CH2), 3.23 (s, 4H, 2CH2). 13C NMR (100 MHz, *DMSO-$d_6$*): 155.64, 115.16, 148.18, 140.71, 129.73, 127.65, 120.79, 113.14, 43.38, 42.65, 42.21. LC-MS (m/z) = 100%, $[M]^+$: 266, $[M+2]^+$: 268. Anal. Calcd. $C_{12}H_{13}Cl_2N_3O_2$ (265.70): C, 47.70; H, 4.34; N, 13.91%. Found C, 47.68; H, 4.38; N, 13.88%.

**General procedure for the synthesis of benzoxazole-piperizine hybrid compounds with amide linkage (*9a-n*)**

At 0 °C, HATU (1.5 eq) was added to a thoroughly mixed solution of the corresponding acid (**8a-n**) (1.0 eq) dissolved in DMF in a nitrogen environment. At room temperature, the mixture was agitated for half an hour. Then, at 0 °C in a nitrogen environment, {1-[(5-chlorobenzo[*d*]oxazol-2-yl)carbonyl]piperazine} [hydrochloride] (**7**) (1.5 eq) and DIPEA (3 eq) were added to the reaction mixture. After then, the reaction was let to continue for 16 more hours at room temperature.[102] TLC was used to track the reaction's development. After finishing, the precipitates were obtained by pouring the reaction mixture into ice-cold water. Acetonitrile and 0.1% formic acid in water were used as the mobile phase in reverse-phase flash chromatography on C18 silica gel (15 µm particle size) to purify the crude precipitates. The relevant desirable products were obtained by vacuum-evaporating the accumulated eluent.

**{4-[(Benzoyl)piperazin-1-yl]-6-chlorobenzo[*d*]oxazol-2-yl}methanone (9a)**

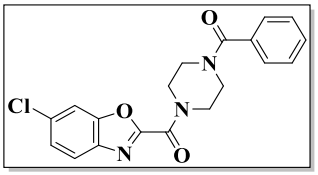

Compound **9a** was prepared from **8a** (0.1 g, 0.82 mmol), HATU (0.470 g, 1.23 mmol) in DMF (2 mL), DIPEA (0.45 mL, 0.317 g, 2.44 mmol), and compound **7** (0.371 g, 1.22 mmol). Off cream solid (0.250 g, 82% yield). mp: 172-175 °C. IR (KBr) $\nu_{max}/cm^{-1}$: 3082 (aromatic-CH), 2922 (aliphatic-CH), 1645 (C=O), 1619 (C=O), 1558 (C=N), 1118 (C-N), 1004 (C-O). $^1$H NMR (400MHz, *DMSO-d$_6$*): δppm 8.06 (s, 1H, Ar-CH), 7.94-7.92 (d, *J* = 8Hz, 2H), 7.64-7.61 (m, 1H, Ar-CH), 7.52-7.42 (m, 5H, Ar-CH (phenyl ring), 4.04 (s, 2H), 3.77 (s, 4H), 3.50 (s, 2H). $^{13}$C NMR (100 MHz, *DMSO-d$_6$*): 169.76, 156.52, 155.92, 148.70, 141.27, 136.00, 130.22, 128.94, 127.94, 127.55, 121.23, 113.57, 46.80, 42.70. LCMS (*m/z*): 99% $[M]^+$:370, $[M+2]^+$: 372. Anal. Calcd. $C_{19}H_{16}ClN_3O_3$ (369.81): C, 61.71; H, 4.36; N, 11.36%. Found C, 61.65; H, 4.40; N, 11.31%.

**(6-chlorobenzo[*d*]oxazol-2-yl)(4-(4-methylbenzoyl)piperazin-1-yl)methanone (9b)**

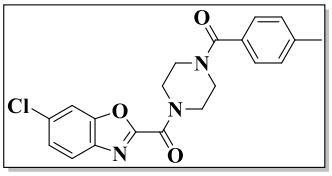

Compound **9b** was prepared from **8b** (0.1 g, 0.73 mmol), HATU (0.418 g, 1.1 mmol) in DMF (2 mL), DIPEA (0.38 mL, 0.284 g, 2.20 mmol) and 7 (0.332 g, 1.10 mmol). Off cream solid (0.220 g, 78% yield). mp: 135-138 °C. IR (KBr) $\nu_{max}/cm^{-1}$: 3080 (aromatic-CH), 2926 (aliphatic-CH), 1645 (C=O), 1617 (C=O), 1556 (C=N), 1121 (C-N), 1004 (C-O). $^1$H NMR (400MHz, *DMSO-d$_6$*): δppm 8.03 (s, 1H, Ar-CH), 7.90-7.88 (d, *J* = 8Hz, 1H, Ar-CH), 7.62-7.59 (m, 1H, Ar-CH), 7.36-7.34 (d, *J* = 8Hz, 2H, 2Ar-CH,), 7.28-7.26 (d, *J* = 8Hz, 2H, 2Ar-CH), 4.01 (s, 2H, $CH_2$), 3.75 (s, 4H, $2CH_2$), 3.60 (s, 2H, $CH_2$), 2.34 (s, 3H, $CH_3$). $^{13}$C NMR (100 MHz, *DMSO-d$_6$*): 169.90, 156.52, 155.93, 141.27, 139.97, 133.03, 130.17, 129.41, 127.95, 127.72, 121.23, 113.57, 46.84, 42.78, 21.40. LC-MS (*m/z*): 98%, $[M]^+$: 384, $[M+1]^+$: 386. Anal. Calcd. $C_{20}H_{18}ClN_3O_3$ (383.83): C, 62.58; H, 4.73; N, 10.95 %. Found C, 62.60; H, 4.70; N, 10.97%.

**(6-chlorobenzo[*d*]oxazol-2-yl)(4-(4-methoxybenzoyl)piperazin-1-yl)methanone (9c)**

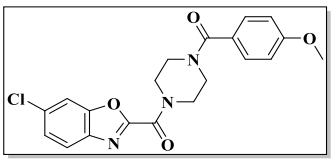

Compound **9c** was prepared from **8c** (0.1 g, 0.65 mmol), HATU (0.372 g, 0.98 mmol) in DMF (2 mL), DIPEA (0.34 mL, 0.253 g, 1.95 mmol) and **7** (0.298 g, 0.98 mmol). Off-cream solid (0.220 g, 83% yield). mp: 127-130 °C. IR (KBr) $\nu_{max}/cm^{-1}$: 3080 (aromatic-CH), 2920 (aliphatic-CH), 1640 (C=O), 1606 (C=O), 1543 (C=N), 1151 (C-N), 1000 (C-O). $^1$H NMR (400MHz, *DMSO-d$_6$*): δppm 8.06 (s, 1H, Ar-CH), 7.94-7.92 (d, *J* = 8Hz, 1H, Ar-CH), 7.64-7.61 (m, 1H, Ar-CH), 7.46-7.42 (d, *J* = 16Hz, 2H, 2Ar-CH), 7.03-7.00 (d, *J* = 12Hz, 2H, 2Ar-CH), 4.03 (s, 2H, $CH_2$), 3.81 (s, 3H, $OCH_3$), 3.77 (s, 2H, $CH_2$), 3.63 (s, 4H, $2CH_2$). $^{13}$C NMR (100 MHz, *DMSO-d$_6$*): 169.72, 160.89, 156.54, 155.93, 148.71, 141.29, 130.17, 129.71, 127.94, 121.24, 114.19, 113.58, 55.78, 46.86, 42.80. LC-MS (*m/z*): 97%, $[M]^+$: 400, $[M+1]^+$: 402. Anal. Calcd. $C_{20}H_{18}ClN_3O_4$ (399.83): C, 60.08; H, 4.54; N, 10.51%. Found C, 60.11; H, 4.51; N, 10.53%.

**(6-chlorobenzo[*d*]oxazol-2-yl)(4-(3,4,5-trimethoxybenzoyl)piperazin-1-yl)methanone (9d)**

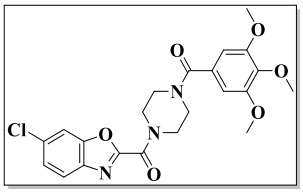

Compound **9d** was prepared from **8d** (0.1 g, 0.47 mmol), HATU (0.268 g, 0.70 mmol) in DMF (2 mL), DIPEA (0.24 mL, 0.182 g, 1.41 mmol) and **7** (0.213 g, 0.70 mmol). Off cream solid (0.180 g, 83% yield). mp: 127-130 °C. IR (KBr) $\nu_{max}/cm^{-1}$: 3093 (aromatic-CH), 2942 (aliphatic-CH), 1654 (C=O), 1612 (C=O), 1552 (C=N), 1123 (C-N), 1012 (C-O). $^1$H NMR (400MHz, *DMSO-d$_6$*): δppm 8.06 (s, 1H, Ar-CH), 7.96-7.92 (m, 1H, Ar-CH), 7.64-7.61 (m, 1H, Ar-CH), 7.75 (s, 2H, 2Ar-CH), 4.04 (s, 2H, $CH_2$), 3.81-3.79 (m, 11H, 3($OCH_3$) $CH_2$), 3.70 (s, 4H, $2CH_2$). $^{13}$C NMR (100 MHz, *DMSO-d$_6$*): 169.41, 156.50, 155.93, 153.27, 148.68, 141.25, 138.83, 131.33, 130.15, 127.94, 121.22, 113.59, 105.02, 60.51, 56.51, 46.86, 42.70. LC-MS (*m/z*): 98%, $[M]^+$: 460, $[M+1]^+$: 462. Anal. Calcd. $C_{22}H_{22}ClN_3O_6$ (459.88): C, 57.46; H, 4.82; N, 9.14%. Found C, 57.42; H, 4.79; N, 9.16%.

**(6-chlorobenzo[*d*]oxazol-2-yl)(4-(4-chlorobenzoyl)piperazin-1-yl)methanone (9e)**

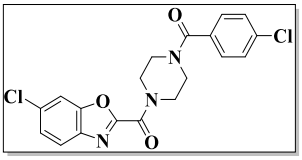

Compound **9e** was prepared from **8e** (0.1 g, 0.63 mmol), HATU (0.361 g, 0.95 mmol) in DMF (2 mL), DIPEA (0.33 mL, 0.245 g, 1.90 mmol) and **7** (0.289 g, 0.95 mmol). Brown solid (0.230 g, 89% yield). mp: 168-170 °C. IR (KBr) $\nu_{max}/cm^{-1}$: 3080 (aromatic-CH), 2935 (aliphatic-CH), 1660 (C=O), 1638 (C=O), 1559 (C=N), 1151 (C-N), 1004 (C-O). $^{1}$H NMR (400MHz, *DMSO-d*$_6$): δppm 8.06 (s, 1H), 7.94-7.92 (d, *J* = 8Hz, 1H), 7.64-7.61 (d, *J* = 12Hz, 1H), 7.56-7.49 (q, *J* = 8.4 Hz, 4H), 4.04 (s, 2H), 3.77 (s, 4H), 3.49 (s, 2H). $^{13}$C NMR (100 MHz, *DMSO-d*$_6$): 168.73, 156.51, 155.91, 148.71, 141.28, 134.93, 134.79, 130.18, 129.61, 129.05, 127.96, 121.23, 113.58, 46.77, 42.71. LC-MS (*m/z*): 100%, $[M]^+$: 404, $[M+1]^+$: 406. Anal. Calcd. $C_{19}H_{15}Cl_2N_3O_3$ (404.25): C, 56.45; H, 3.74; N, 10.39%. Found C, 56.42; H, 3.70; N, 10.43%.

**(4-(4-bromobenzoyl)piperazin-1-yl)(6-chlorobenzo[*d*]oxazol-2-yl)methanone (9f)**

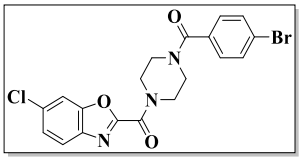

Compound **9f** was prepared from **8f** (0.1 g, 0.49 mmol), HATU (0.281 g, 0.74 mmol) in DMF (2 mL), DIPEA (0.25 mL, 0.191 g, 1.48 mmol) and **7** (0.225 g, 0.74 mmol). Off white solid (0.190 g, 85% yield). mp: 172-175 °C. IR (KBr) $\nu_{max}/cm^{-1}$: 3082 (aromatic-CH), 2918 (aliphatic-CH), 1653 (C=O), 1634 (C=N), 1533 (C=C), 1146 (C-N), 1002 (C-O). $^{1}$H NMR (400MHz, *DMSO-d*$_6$): δppm 8.06 (s, 1H, Ar-CH), 7.94-7.92 (d, *J* = 8Hz, 1H, Ar-CH), 7.69-7.61 (m, 3H, 3Ar-CH), 7.44-7.42 (d, *J* = 8Hz, 2H, 2Ar-CH), 4.05 (s, 2H, $CH_2$), 3.76 (s, 4H, $2CH_2$), 3.51-3.46 (m, 2H, $CH_2$). $^{13}$C NMR (100 MHz, *DMSO-d*$_6$): 168.74, 156.47, 155.87, 148.67, 141.25, 135.12, 131.95, 130.15, 129.81, 127.95, 123.63, 121.23, 113.59, 46.96, 42.54. LC-MS (*m/z*): 98%, $[M]^+$: 448, $[M+1]^+$: 450. Anal. Calcd. $C_{19}H_{15}BrClN_3O_3$ (448.70): C, 50.86; H, 3.37; N, 9.37%. Found C, 50.83; H, 3.40; N, 9.41%.

**(6-chlorobenzo[*d*]oxazol-2-yl)(4-(4-fluorobenzoyl)piperazin-1-yl)methanone (9g)**

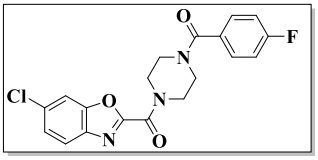

Compound **9g** was prepared from **8g** (0.1 g, 0.71 mmol), HATU (0.406 g, 1.07 mmol) in DMF (2 mL), DIPEA (0.37 mL, 0.276 g, 2.14 mmol) and **7** (0.323 g, 1.07 mmol). Off cream solid (0.250 g, 90% yield). mp: 199-202 °C. IR (KBr) $\nu_{max}/cm^{-1}$: 3080 (aromatic-CH), 2920 (aliphatic-CH), 1645 (C=O), 1621 (C=O), 1558 (C=N), 1120 (C-N), 1002 (C-O). $^1$H NMR (400MHz, *DMSO-d₆*): δppm 8.02 (s, 1H, Ar-CH), 7.90-7.88 (d, *J* = 8Hz, 1H, Ar-CH), 7.62-7.59 (m, 1H, Ar-CH), 7.55-7.51 (t, *J* = 8Hz, 2H, 2$CH_2$), 7.31-7.27 (t, *J* = 8Hz, 2H, 2Ar-CH), 4.02 (s, 2H, $CH_2$), 3.85-3.60 (m, 6H, 3$CH_2$). $^{13}$C NMR (100 MHz, *DMSO-d₆*): 168.89, 164.40, 161.94, 156.52, 155.92, 148.71, 141.28, 132.39, 130.27, 130.18, 127.95, 121.23, 116.02, 115.81, 113.57, 46.78, 42.71. LC-MS (*m/z*): 99%, $[M]^+$: 388, $[M+2]^+$: 390. Anal. Calcd. $C_{19}H_{15}ClFN_3O_3$ (387.80): C, 58.85; H, 3.90; N, 10.84%. Found C, 58.89; H, 3.88; N, 10.86%.

**(6-chlorobenzo[*d*]oxazol-2-yl)(4-(4-nitrobenzoyl)piperazin-1-yl)methanone (9h)**

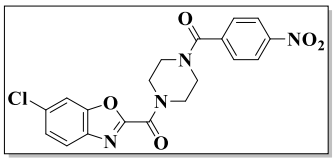


Compound **9h** was prepared from **8h** (0.1 g, 0.59 mmol), HATU (0.338 g, 0.89 mmol) in DMF (2 mL), DIPEA (0.31 mL, 0.231 g, 1.79 mmol) and 7 (0.269 g, 0.89 mmol). Off cream solid (0.220 g, 88% yield). mp: 230-233 °C. IR (KBr) $\nu_{max}/cm^{-1}$: 3058 (aromatic-CH), 2957 (aliphatic-CH), 1645 (C=O), 1623 (C=O), 1526 (C=N), 1161 (C-N), 1004 (C-O). $^1$H NMR (400MHz, *DMSO-d₆*): δppm 8.32 (s, 1H, Ar-CH), 8.09-8.00 (d, *J* = 8Hz, 1H, Ar-CH), 7.98 (s, 1H, Ar-CH), 7.76-7.74 (d, *J* = 7.6Hz, 2H, 2Ar-CH), 7.63 (s, 1H, Ar-CH), 4.12-4.00 (m, 2H, $CH_2$), 3.85-3.70 (m, 4H, 2$CH_2$), 3.43 (s, 2H, $CH_2$). $^{13}$C NMR (100 MHz, *DMSO-d₆*): 167.88, 162.28, 156.46, 155.90, 148.69, 148.40, 142.31, 141.25, 130.17, 128.93, 127.98, 124.28, 121.24, 113.58, 46.86, 42.79. LC-MS (*m/z*): 100%, $[M]^+$: 415, $[M+2]^+$: 417. Anal. Calcd. $C_{19}H_{15}ClN_4O_5$ (414.80): C, 55.02; H, 3.65; N, 13.51%. Found C, 55.06; H, 3.68; N, 13.53%.

**(6-chlorobenzo[*d*]oxazol-2-yl)(4-(4-(trifluoromethyl)benzoyl)piperazin-1-yl)methanone (9i)**

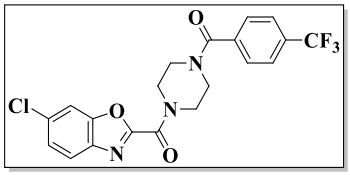


Compound **9i** was prepared from **8i** (0.1 g, 0.52 mmol), HATU (0.300 g, 0.79 mmol) in DMF (2 mL), DIPEA (0.27 mL, 0.204 g, 1.58 mmol) and **7** (0.238 g, 0.79 mmol). Off

white solid (0.180 g, 78% yield). mp: 167-171 °C. IR (KBr) $\nu_{max}/cm^{-1}$: 3015 (aromatic-CH), 2924 (aliphatic-CH), 1643 (C=O), 1617 (C=O), 1558 (C=N), 1121 (C-N), 1002 (C-O). $^1$H NMR (400MHz, *DMSO-d₆*): δppm 8.15-7.95 (m, 1H, Ar-CH), 7.94-7.92 (d, *J* = 8Hz, 1H, Ar-CH), 7.85 (s, 2H, 2Ar-CH), 7.71-7.69 (d, *J* = 8Hz, 2H, 2Ar-CH), 7.64-7.62 (d, *J* = 8Hz, 1H, Ar-CH), 4.15-3.95 (m, 2H, $CH_2$), 3.88-3.65 (m, 4H, $2CH_2$), 3.45 (s, 2H, $CH_2$). $^{13}$C NMR (100 MHz, *DMSO-d₆*): 168.37, 156.46, 155.88, 148.67, 141.24, 140.12, 130.15, 128.38, 127.96, 126.01, 121.21, 113.59, 46.94, 42.36. LC-MS (*m/z*): 97%, $[M]^+$: 438, $[M+2]^+$: 440. Anal. Calcd. $C_{20}H_{15}ClF_3N_3O_3$ (437.80): C, 54.87; H, 3.45; N, 9.60%. Found C, 54.91; H, 3.49; N, 9.64%.

**(4-(4-bromo-2-iodobenzoyl)piperazin-1-yl)(6-chlorobenzo[*d*]oxazol-2-yl)methanone (9j)**

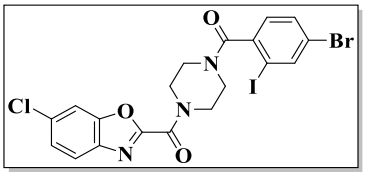


Compound **9j** was prepared from **8j** (0.1 g, 0.30 mmol), HATU (0.174 g, 0.46 mmol) in DMF (2 mL), DIPEA (0.16 mL, 0.119 g, 0.92 mmol), **7** (0.138 g, 0.46 mmol). Off cream solid (0.125 g, 71% yield). mp: 187-191 °C. IR (KBr) $\nu_{max}/cm^{-1}$: 3073 (aromatic-CH), 2924 (aliphatic-CH), 1654 (C=O), 1602 (C=O), 1545 (C=N), 1155 (C-N), 1002 (C-O). $^1$H NMR (400MHz, *DMSO-d₆*): δppm 8.16-8.01 (m, 2H, 2Ar-CH), 7.96-7.92 (t, *J* = 8Hz, 1H, Ar-CH), 7.75-7.70 (m, 1H, Ar-CH), 7.66-7.61 (m, 1H, Ar-CH), 7.33-7.29 (m, 1H, Ar-CH), 4.12-4.03 (m, 2H, $CH_2$), 3.88-3.69 (m, 4H, $2CH_2$), 3.34-3.25 (m, 2H, $CH_2$). $^{13}$C NMR (100 MHz, *DMSO-d₆*): 168.28, 156.42, 155.90, 148.69, 148.66, 141.48, 141.26, 141.21, 140.87, 140.81, 132.00, 130.17, 129.25, 127.98, 122.90, 121.30, 121.15, 113.59, 95.06, 48.88, 42.37. LC-MS (*m/z*): 96%, $[M]^+$: 574, $[M+2]^+$: 576. Anal. Calcd. $C_{19}H_{14}BrClIN_3O_3$ (574.60): C, 39.72; H, 2.46; N, 7.31%. Found C, 39.75; H, 2.48; N, 7.34%.

**(4-(4-bromo-2,6-difluorobenzoyl)piperazin-1-yl)(6-chlorobenzo[*d*]oxazol-2-yl)methanone (9k)**

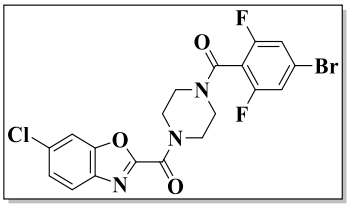

Compound **9k** was prepared from **8k** (0.1 g, 0.42 mmol), HATU (0.239 g, 0.63 mmol) in DMF (2 mL), DIPEA (0.21 mL, 0.162 g, 1.26 mmol) and **7** (0.190 g, 0.63 mmol). Cream solid (0.150 g, 73% yield), mp: 160-164 °C. IR (KBr) $\nu_{max}/cm^{-1}$: 3080 (aromatic-CH), 2920 (aliphatic-CH), 1638 (C=O), 1615 (C=O), 1541 (C=N), 1157 (C-N), 1004 (C-O). $^1$H NMR (400MHz, *DMSO-d6*): δppm 8.11-8.02 (m, 1H, Ar-CH), 7.96-7.92 (m, 1H, Ar-CH), 7.72-7.61 (m, 3H, 3Ar-CH), 4.14-4.10 (t, *J* = 8Hz, 1H, CH), 4.00-3.97 (m, 1H, CH), 3.81-3.76 (m, 3H, CH2, CH), 3.70-3.67 (m, 1H, CH), 3.50-3.46 (m, 2H, $CH_2$). $^{13}$C NMR (100 MHz, *DMSO-d6*): 159.40, 159.31, 158.55, 156.90, 156.81, 155.92, 155.36, 155.29, 148.18, 140.79, 179.72, 127.57, 123.26, 120.85, 120.69, 116.36, 116.11, 113.14, 112.70, 46.24, 41.72. LC-MS (*m/z*): 94%, $[M]^+$: 484, $[M+2]^+$: 486. Anal. Calcd. $C_{19}H_{13}BrClF_2N_3O_3$ (484.68): C, 47.08; H, 2.70; N, 8.67%. Found C, 47.10; H, 2.72; N, 8.64%.

**(4-(4-bromo-2-(trifluoromethyl)benzoyl)piperazin-1-yl)(6-chlorobenzo[*d*]oxazol-2-yl)methanone (9l)**

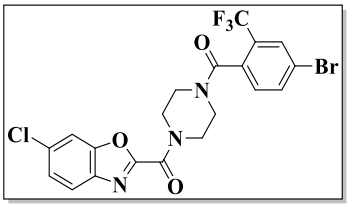


Compound **9l** was prepared from **8l** (0.1 g, 0.37 mmol), HATU (0.209 g, 0.55 mmol) in DMF (2 mL), DIPEA (0.19 mL, 0.142 g, 1.10 mmol) and **7** (0.168 g, 0.55 mmol). Off orange solid (0.160 g, 83% yield). mp: 129-132 °C. IR (KBr) $\nu_{max}/cm^{-1}$: 3075 (aromatic-CH), 2920 (aliphatic-CH), 1641 (C=O), 1593 (C=O), 1565 (C=N), 1131 (C-N), 1006 (C-O). $^1$H NMR (400MHz, *DMSO-d6*): δppm 8.11-8.08 (m, 1H, Ar-CH), 8.06-7.99 (m, 2H, 2Ar-CH), 7.96-7.91 (m, 1H, Ar-CH), 7.65-7.58 (m, 1H, Ar-CH), 7.57-7.55 (m, 1H, Ar-CH), 4.09 (m, 1H, CH), 4.00-3.73 (m, 3H, $CH_2$, CH), 3.72-3.55 (m, 2H,$CH_2$), 3.30-3.15 (m, 2H, $CH_2$). $^{13}$C NMR (100 MHz, *DMSO-d6*): 196.83, 165.96, 156.42, 155.83, 148.68, 141.25, 136.49, 134.04, 130.21, 129.88, 127.98, 124.58, 123.07, 123.00, 121.86, 121.29, 121.12, 113.58, 46.67, 41.98. LC-MS (*m/z*): 99%, $[M]^+$: 516, $[M+2]^+$: 518. Anal. Calcd. $C_{20}H_{14}BrClF_3N_3O_3$ (516.70): C, 46.49; H, 2.73; N, 8.13%. Found C, 46.52; H, 2.76; N, 8.17%.

**(4-(4-bromo-2-nitrobenzoyl)piperazin-1-yl)(6-chlorobenzo[*d*]oxazol-2-yl)methanone (9m)**

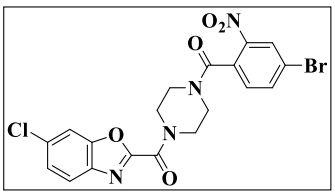

Compound **9m** was prepared from **8m** (0.1 g, 0.40 mmol), HATU (0.209 g, 0.60 mmol) in DMF (2 mL), DIPEA (0.21 mL, 0.157 g, 1.22 mmol) and **7** (0.181 g, 0.60 mmol). Off cream solid (0.190 g, 94% yield). mp: 147-150 °C. IR (KBr) $\nu_{max}/cm^{-1}$: 3082 (aromatic-CH), 2924 (aliphatic-CH), 1653 (C=O), 1627 (C=O), 1530 (C=N), 1157 (C-N), 1000 (C-O). $^1$H NMR (400MHz, *DMSO-d$_6$*): δppm 8.45-8.42 (m, 1H, Ar-CH), 8.14-7.99 (m, 2H, 2Ar-CH), 7.96-7.91 (m, 1H, Ar-CH), 7.65-7.58 (m, 2H, 2Ar-CH), 4.12 (s, 1H, CH), 3.96 (s, 1H, CH), 3.87-3.68 (m, 4H, 2CH$_2$), 3.46-3.44 (m, 2H, CH$_2$). $^{13}$C NMR (100MHz, *DMSO-d$_6$*): 165.32, 156.46, 155.92, 155.82, 148.66, 146.60, 141.22, 138.16, 131.51, 130.33, 130.17, 128.00, 123.01, 121.30, 121.12, 113.59, 46.80, 42.13. LC-MS (*m/z*): 98%, $[M]^+$: 493, $[M+2]^+$: 495. Anal. Calcd. $C_{19}H_{14}BrClN_4O_5$ (493.70): C, 46.22; H, 2.86; N, 11.35%. Found C, 46.25; H, 2.90; N, 11.38%.

**(6-chlorobenzo[*d*]oxazol-2-yl)(4-(4-methoxy-2-nitrobenzoyl)piperazin-1-yl)methanone (9n)**

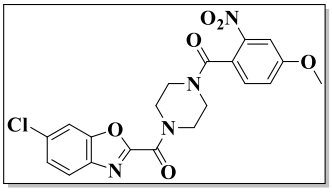

Compound **9n** was prepared from **8n** (0.1 g, 0.51 mmol), HATU (0.289 g, 0.76 mmol) in DMF (2 mL), DIPEA (0.26 mL, 0.196 g, 1.52 mmol) and 7 (0.230 g, 0.76 mmol). Off cream solid (0.215 g, 95% yield). mp: 197-200 °C. IR (KBr) $\nu_{max}/cm^{-1}$: 3089 (aromatic-CH), 2924 (aliphatic-CH), 1660 (C=O), 1630 (C=O), 1565 (C=N), 1142 (C-N), 1000 (C-O). $^1$H NMR (400MHz, *DMSO-d$_6$*): δppm 8.11-7.96 (m, 1H, Ar-CH), 7.94-7.91 (m, 2H, 2Ar-CH), 7.96-7.91 (m, 1H, Ar-CH), 7.72-7.69 (m, 1H, Ar-CH), 7.65-7.58 (m, 1H, Ar-CH), 7.55-7.52 (m, 1H, Ar-CH), 7.48-7.42 (m, 1H, Ar-CH), 4.11 (s, 1H, CH), 3.96-3.90 (m, 4H, CH$_3$, CH), 3.83 (s, 1H, CH), 3.80-3.75 (m, 2H, CH$_2$), 3.69 (s, 1H, CH), 3.39-3.37 (m, 2H, CH$_2$). $^{13}$C NMR (100 MHz, *DMSO-d$_6$*): 166.18, 160.38, 156.48, 148.71, 147.26, 141.29, 130.18, 129.76, 127.98, 124.59, 121.30, 121.14, 121.04, 113.58, 110.20, 56.72, 46.82, 42.16. LC-MS (*m/z*): 96%, $[M]^+$: 445, $[M+2]^+$:

447. Anal. Calcd. $C_{20}H_{17}ClN_4O_6$ (444.83): C, 54.00; H, 3.85; N, 12.60%. Found C, 53.96; H, 3.87; N, 12.64%.

### 2.8.2 Protocol of Antimicrobial Activity

Along with strains of two gram-positive (*Bacillus subtilis* and *Staphylococcus aureus*) and two gram-negative (*Pseudomonas aeruginosa* and *Escherichia coli*) bacteria, the antibacterial and antifungal activity was tested against the common fungal pathogens *Aspergillus niger* and *Candida albicans*. The inhibition zone (mm) of nutrient agar with the composition (gL-1): Sodium chloride, 5.0; Beef extract, 10.0; Peptone, 10.0 was tested using the antibacterial and antifungal standards Chloramphenicol (30 µg/disc), Gentamicin (10 µg/disc), and Nystatin (10 µg/disc), respectively. The medium was brought to a pH of 7.2 prior to sterilization.[109] The experimental results showed that the investigated chemicals strongly inhibited all bacterial strains, with an inhibition zone ranging from 10 to 36 mm and an inhibition zone ranging from 11 to 30 mm for fungal species. In comparison to reference medications, the synthesized molecule exhibited a greater and more moderate activity. The antibacterial activity of the investigated chemical was assessed using a molecule's 10 µg/disc attentiveness in DMSO.

### 2.8.3 Protocol of Molecular Docking Study

*E. Coli* DNA gyrase B (PDB: 4DUH) high-resolution crystal structures were obtained from the PDB database (https://www.rcsb.org/). In order to ensure that the docking investigation was unaffected by extraneous entities, the protein receptors were prepared for molecular docking by removing water molecules and associated ligands using Discovery Studio Visualizer (v21.1.0). Empirical force fields were then used to minimize energy and create lower-energy protein conformations.[112] Using AutoDock (v4.2) virtual screening software, molecular docking analysis was performed, treating the chemicals as ligand molecules and the 4DUH protein as the macromolecules. For 4DUH, a cubic grid box measuring 72.77 × 47.35 × 62.99 was constructed. Eight separate docking runs were performed on each compound, and conformations were grouped according to an RMSD of less than 2.0 Å.[113] The lowest free binding energy (in kcal/mol) was used to determine each compound's optional binding configuration. Discovery Studio Visualizer (v21.1.0) was used to evaluate molecular interactions and offer comprehensive information about the binding profiles.

### 2.8.4 Protocol of Molecular Dynamic Simulation

Using Desmond software from Schrodinger LLC, a 100-nanosecond MDS was carried out.[114] Protein-ligand docking was performed before starting MDS to ascertain how the molecule would stay positioned inside the protein's active site. By simulating atomic motions over time using Newton's classical equations of motion, MDS offers comprehensive insights into the dynamics of ligand-binding in a physiological setting.[115] Using Maestro's Protein Preparation Wizard, the ligand-receptor complex was pre-processed, encompassing energy minimization, optimization, and, if necessary, resolving any missing residues. The System Builder tool was then used to prepare the system. The models were relaxed before the simulation was conducted, and trajectories were captured for in-depth examination at 100 ps intervals.

### 2.8.5 Protocol of ADMET Study

The Swiss Institute of Bioinformatics (SIB) developed SwissADME, a free web application that forecasts small compounds' Absorption, Distribution, Metabolism, and Excretion (ADME) characteristics. It is frequently employed to evaluate pharmacokinetics and other drug-like properties.[114]

## 2.9 Conclusion

Using $^{1}$H NMR, $^{13}$C NMR, LC-MS, and IR spectrum analysis, a new series of hybrid molecules comprising benzoxazole derivatives with substituted piperazine moieties was created and examined. The bactericidal qualities of each produced molecule were assessed. Excellent antibacterial activity against both gram-positive and gram-negative infections was demonstrated by the majority of the recently produced drugs. Compounds **9f** and **9b**, which had the highest docking scores of -7.8 kcal/mol and -7.7 kcal/mol, respectively, showed the most promising findings in antibacterial activity among the synthesized compounds. With a docking score of -7.5 kcal/mol, compounds **9c**, **9i**, and **9n** demonstrated modest antibacterial activity. Furthermore, compound **9f**'s antibacterial efficacy may be due to its inhibition of *E. coli* DNA gyrase, according to molecular docking and molecular dynamics simulations. With the exception of compounds **9k** and **9l**, which had molecular weights more than 500, all produced compounds adhered to Lipinski's rule of five. Interestingly, the lipophilicity ratings of

all benzoxazole derivatives ranged from 1.94 to 4.31. Using SwissADME, the computational analysis was carried out.

## 2.10 Representative spectral data

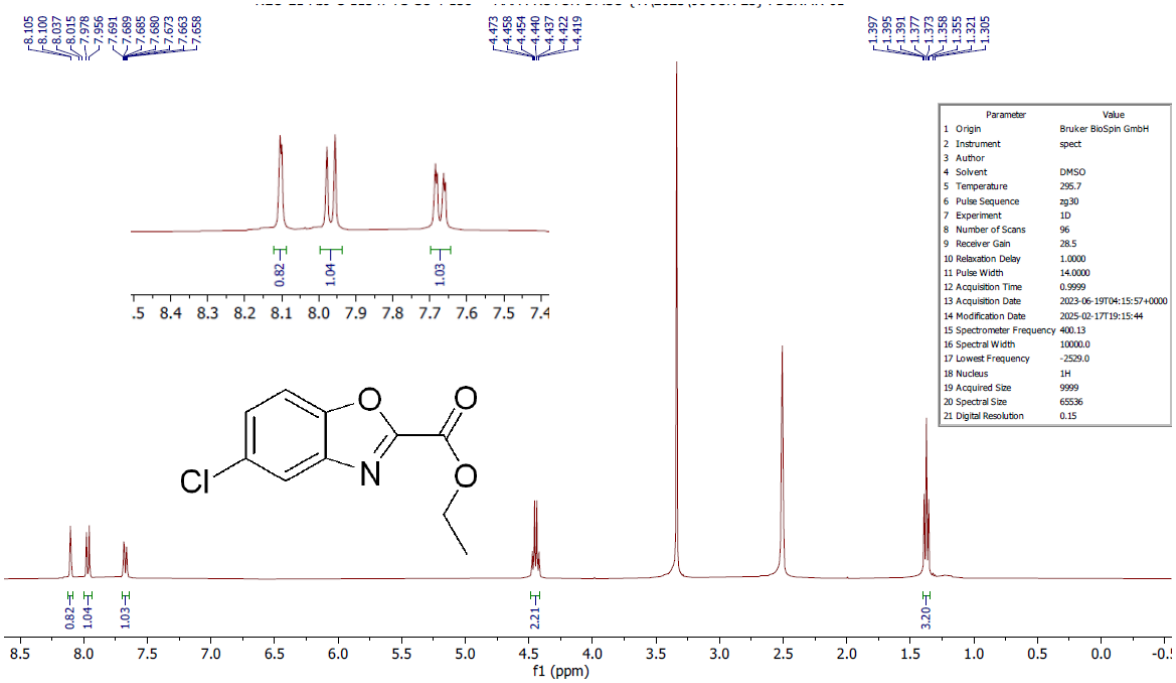


**Figure 19:** $^{1}$H NMR of compound **4.**

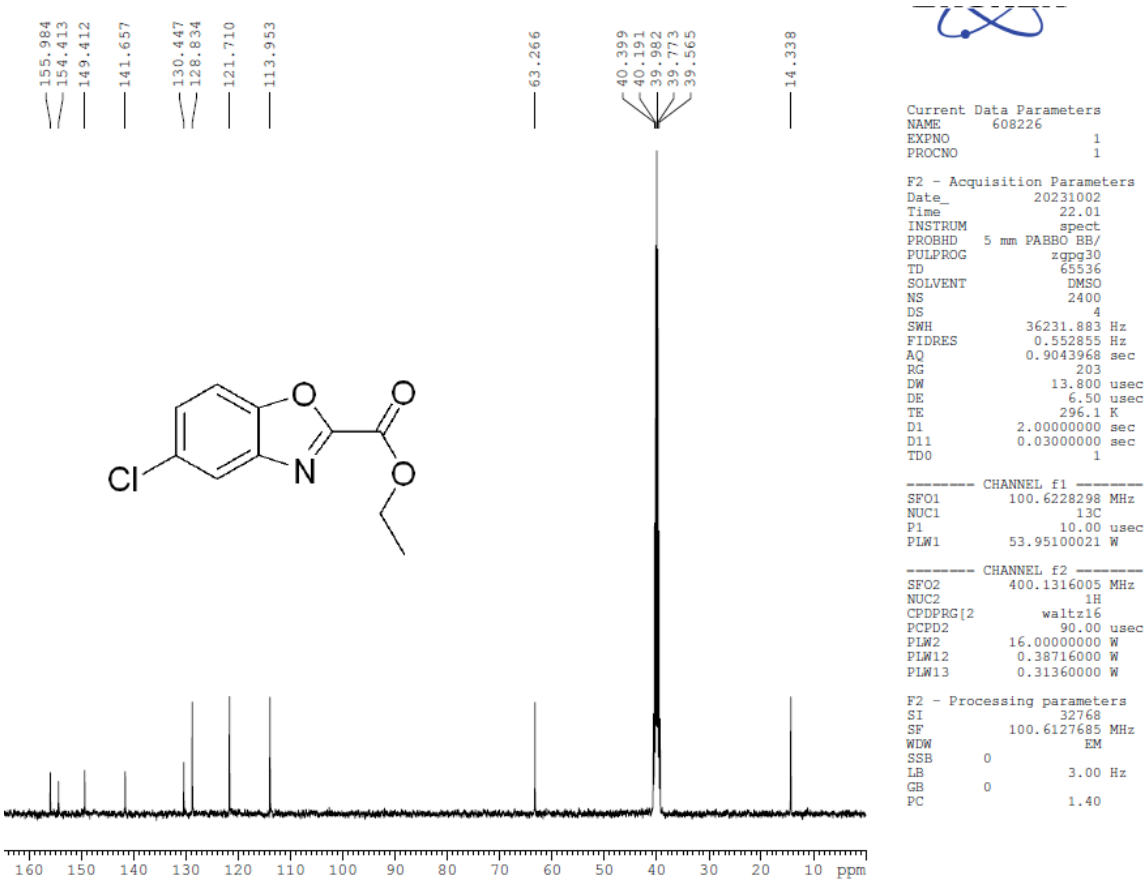


**Figure 20:** $^{13}$C NMR of compound **4.**

| | | | |
|---|---|---|---|
| Sample Name: | | | |
| Sample Type: | Unknown | Acquired By: | LCMS_03 |
| Vial: | 2:A,7 | Sample Set Name: | 17062023_UCH_177 |
| Injection #: | 1 | Acq. Method Set: | PDS_METHOD_C |
| Injection Volume: | 1.00 ul | Processing Method: | PDS_METHOD_C_03, |
| Run Time: | 3.0 Minutes | Channel Name: | 220.0nm, MS TIC, 254.0nm |
| Project Name | LCMS-03_JUN-2023_17062023 | Proc. Chnl. Descr.: | SQ 3: MS Scan MS TIC, PDA |
| Date Acquired: | 17-06-2023 20:32:43 IST | | |
| Date Processed: | 17-06-2023 21:00:28 IST, 17-06-2023 21:00:42 IST, 17-06-2023 21:01:20 IST, 17-06-2023 | | |

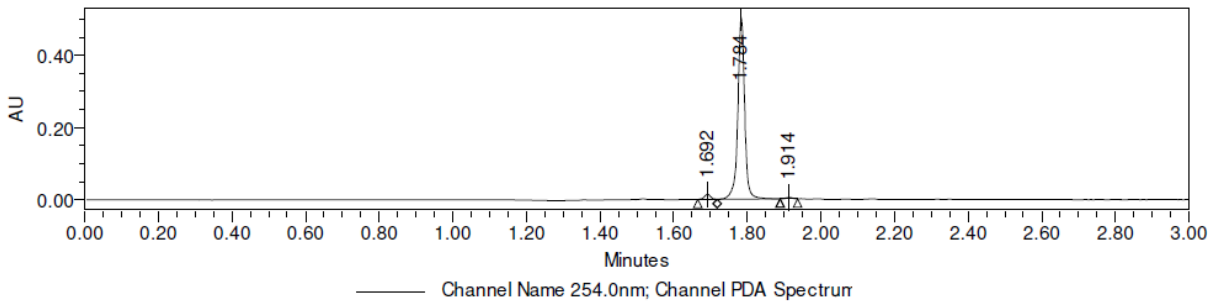

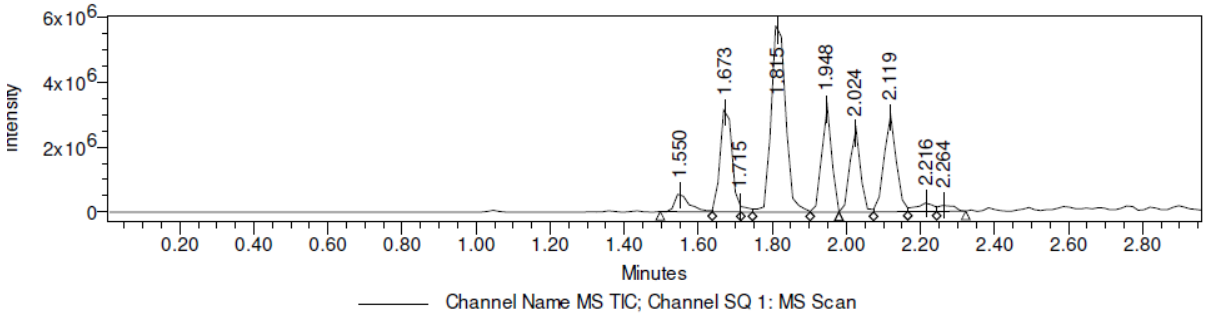


Channel: PDA Spectrum

| | Retention Time (min) | Base Peak (m/z) | Height (µV) | Area (µV*sec) | % Area | Channel | Channel Name |
|---|---|---|---|---|---|---|---|
| 1 | 1.530 | | 6952 | 18860 | 2.92 | PDA Spectrum | 220.0nm |
| 2 | 1.638 | | 9813 | 20665 | 3.20 | PDA Spectrum | 220.0nm |
| 3 | 1.692 | | 13492 | 15268 | 2.27 | PDA Spectrum | 254.0nm |
| 4 | 1.693 | | 14839 | 23365 | 3.62 | PDA Spectrum | 220.0nm |
| 5 | 1.784 | | 388989 | 527273 | 81.66 | PDA Spectrum | 220.0nm |
| 6 | 1.784 | | 504167 | 653443 | 97.09 | PDA Spectrum | 254.0nm |
| 7 | 1.823 | | 9194 | 21778 | 3.37 | PDA Spectrum | 220.0nm |
| 8 | 1.914 | | 3951 | 4344 | 0.65 | PDA Spectrum | 254.0nm |
| 9 | 1.915 | | 12386 | 20095 | 3.11 | PDA Spectrum | 220.0nm |
| 10 | 1.940 | | 6006 | 7228 | 1.12 | PDA Spectrum | 220.0nm |
| 11 | 1.987 | | 4411 | 6456 | 1.00 | PDA Spectrum | 220.0nm |

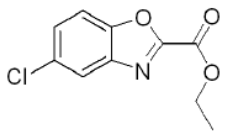


Chemical Formula: $C_{10}H_8ClNO_3$
Molecular Weight: 225.63

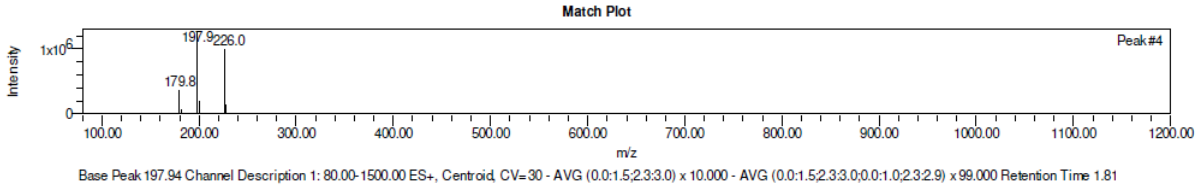


**Figure 21:** LC-MS of compound **4.**

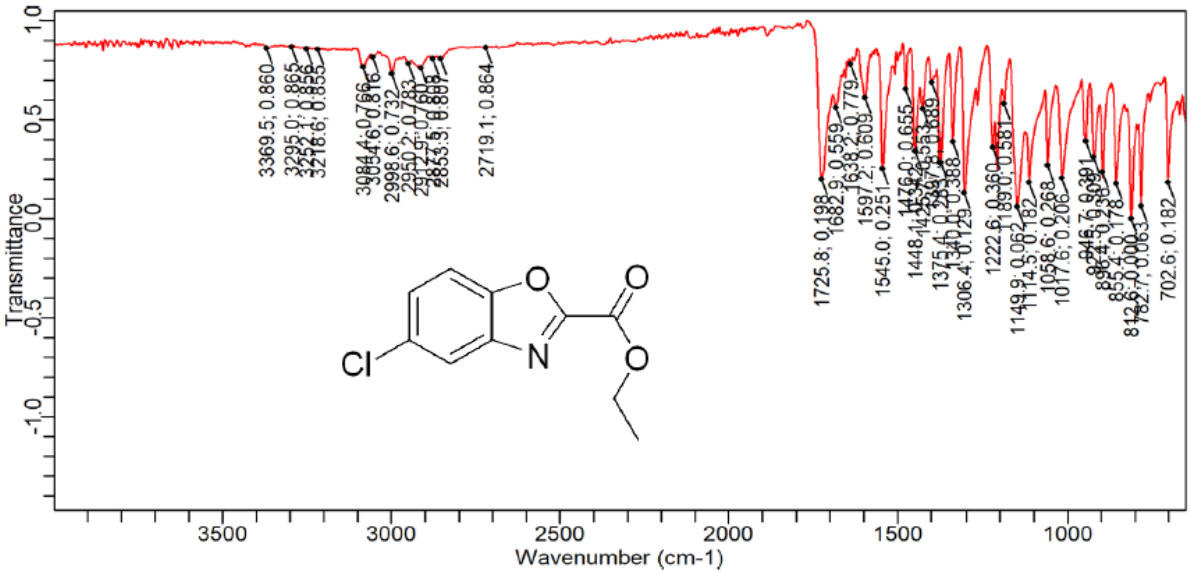


**Figure 22:** IR of compound **4.**

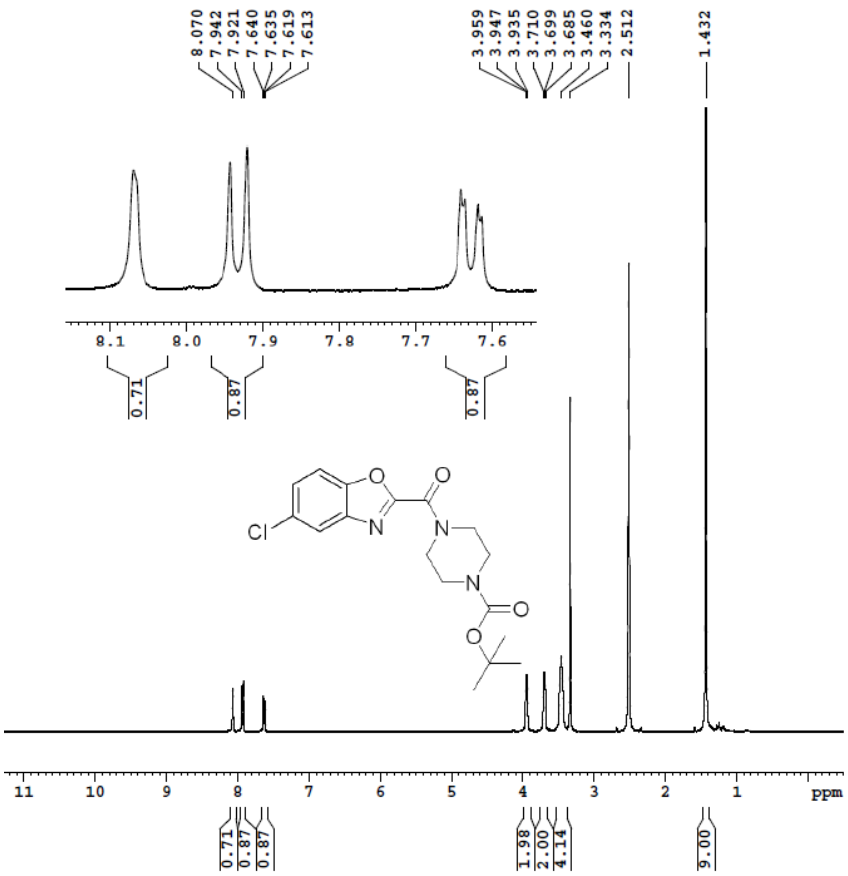


```
Current Data Parameters
NAME       611114
EXPNO           1
PROCNO          1

F2 - Acquisition Parameters
Date_        20231004
Time            13.09 h
INSTRUM         spect
PROBHD   Z108618_0769 (
PULPROG         zg30
TD             16384
SOLVENT         DMSO
NS                16
DS                 0
SWH          8012.820 Hz
FIDRES       0.978127 Hz
AQ          1.0223616 sec
RG             201.52
DW             62.400 usec
DE              6.50 usec
TE             337.5 K
D1          1.00000000 sec
TD0                1
SFO1       400.3024720 MHz
NUC1               1H
P0              5.00 usec
P1             15.00 usec
PLW1       14.00000000 W

F2 - Processing parameters
SI             65536
SF         400.2999993 MHz
WDW               EM
SSB                0
LB              0.30 Hz
GB                 0
PC              1.00
```

**Figure 23:** $^{1}$H NMR of compound **6.**

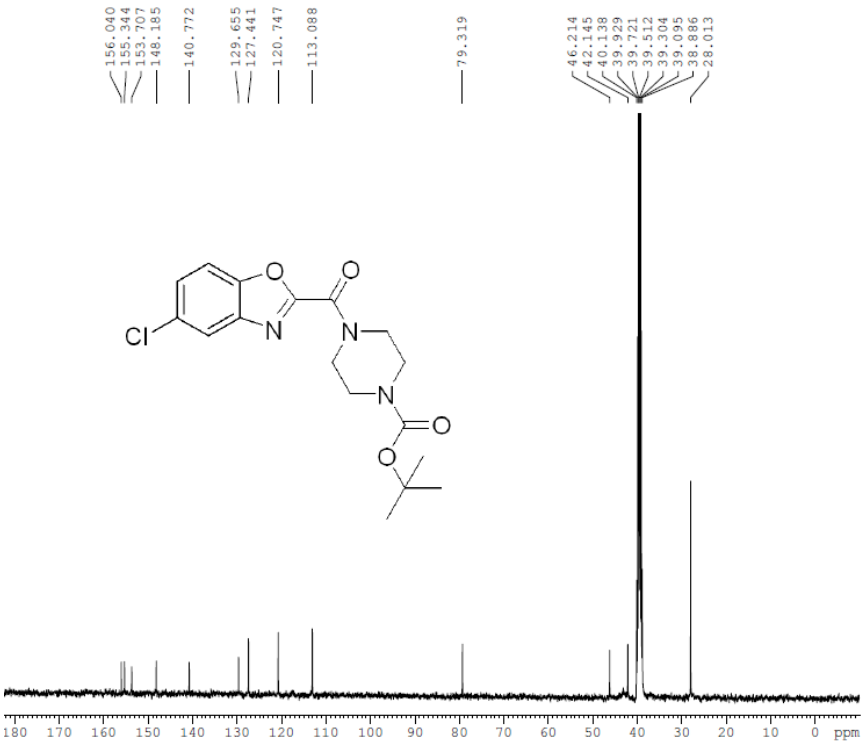


```
Current Data Parameters
NAME       611088
EXPNO           1
PROCNO          1

F2 - Acquisition Parameters
Date_        20231004
Time            13.19
INSTRUM         spect
PROBHD   5 mm PABBO BB/
PULPROG        zgpg30
TD             65536
SOLVENT         DMSO
NS               256
DS                 4
SWH         24038.461 Hz
FIDRES       0.366798 Hz
AQ          1.3631488 sec
RG               203
DW             20.800 usec
DE              6.50 usec
TE             296.2 K
D1          2.00000000 sec
D11         0.03000000 sec
TD0                1

======== CHANNEL f1 ========
SFO1       100.6228293 MHz
NUC1              13C
P1             10.00 usec
PLW1       53.95100021 W

======== CHANNEL f2 ========
SFO2       400.1316005 MHz
NUC2               1H
CPDPRG[2        waltz16
PCPD2          90.00 usec
PLW2       16.00000000 W
PLW12       0.38716000 W
PLW13       0.31360000 W

F2 - Processing parameters
SI             32768
SF         100.6128160 MHz
WDW               EM
SSB                0
LB              3.00 Hz
GB                 0
PC              1.40
```

**Figure 24:** $^{13}$C NMR of compound **6.**

Sample Name:

| | | | |
|---|---|---|---|
| Sample Type: | Unknown | Acquired By: | LCMS-02 |
| Vial: | 1:A,3 | Sample Set Name: | 25062023_UCH 128_1ST |
| Injection #: | 1 | Acq. Method Set: | METHOD C3 |
| Injection Volume: | 1.00 ul | Processing Method: | LCMS METHOD J2_02, |
| Run Time: | 3.0 Minutes | Channel Name: | 230.0nm, MS TIC, 254.0nm, |
| Project Name | LCMS-02_JUNE-2023_25062023 | Proc. Chnl. Descr.: | PDA 290.0 nm Blank Subtracted |
| Date Acquired: | 25-06-2023 12:52:24 IST | | |
| Date Processed: | 25-06-2023 13:31:16 IST, 25-06-2023 13:31:25 IST, 25-06-2023 13:31:41 IST, 25-06-2023 | | |

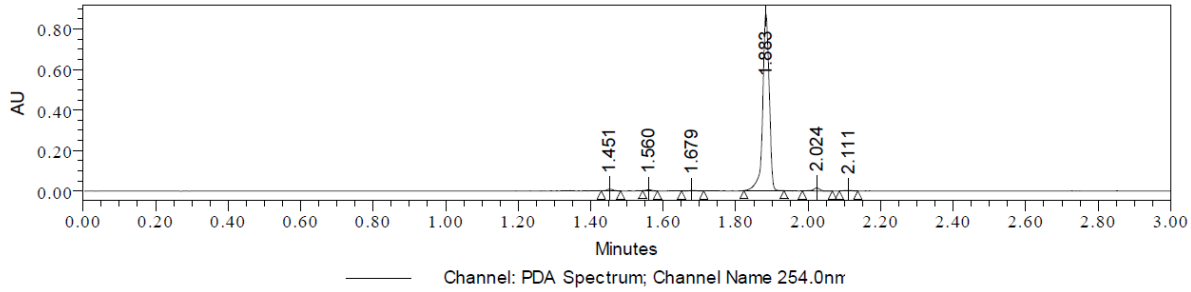


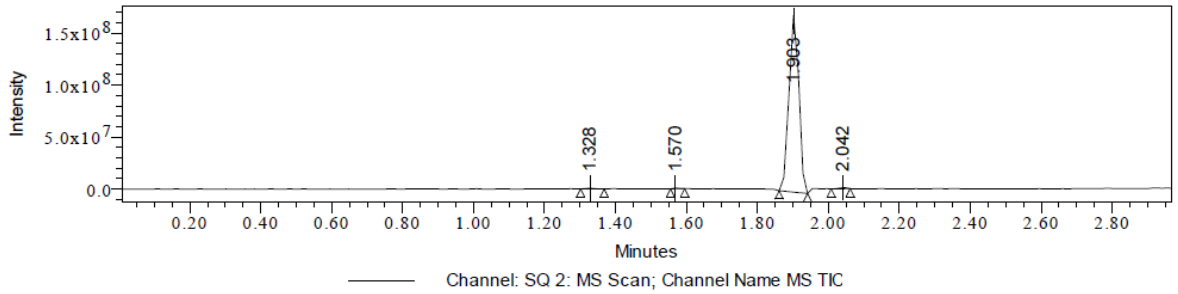


**Channel: PDA Spectrum**

| | Retention Time (min) | Base Peak (m/z) | Height (µV) | Area (µV*sec) | % Area | Channel | Channel Name |
|---|---|---|---|---|---|---|---|
| 1 | 1.346 | | 6008 | 6137 | 0.67 | PDA Spectrum | 230.0nm |
| 2 | 1.451 | | 9389 | 8850 | 0.96 | PDA Spectrum | 230.0nm |
| 3 | 1.451 | | 8310 | 9756 | 0.86 | PDA Spectrum | 254.0nm |
| 4 | 1.452 | | 5159 | 5344 | 0.59 | PDA Spectrum | 290.0nm |
| 5 | 1.560 | | 5115 | 5759 | 0.51 | PDA Spectrum | 254.0nm |
| 6 | 1.560 | | 8803 | 16314 | 1.77 | PDA Spectrum | 230.0nm |
| 7 | 1.621 | | 4750 | 5424 | 0.59 | PDA Spectrum | 230.0nm |
| 8 | 1.679 | | 1834 | 2175 | 0.19 | PDA Spectrum | 254.0nm |
| 9 | 1.883 | | 704495 | 889086 | 98.69 | PDA Spectrum | 290.0nm |
| 10 | 1.883 | | 677011 | 856952 | 93.15 | PDA Spectrum | 230.0nm |
| 11 | 1.883 | | 873020 | 1093607 | 96.62 | PDA Spectrum | 254.0nm |
| 12 | 2.022 | | 6529 | 6492 | 0.72 | PDA Spectrum | 290.0nm |
| 13 | 2.024 | | 14671 | 17313 | 1.53 | PDA Spectrum | 254.0nm |
| 14 | 2.025 | | 21690 | 26307 | 2.86 | PDA Spectrum | 230.0nm |
| 15 | 2.111 | | 2316 | 3280 | 0.29 | PDA Spectrum | 254.0nm |

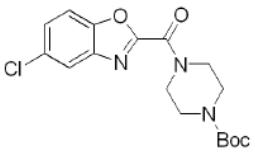


Chemical Formula: $C_{17}H_{20}ClN_3O_4$
Molecular Weight: 365.81

M-56 mass observed

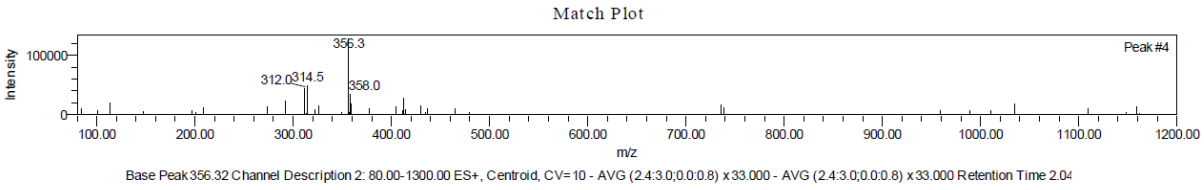


**Figure 25:** LC-MS of compound **6.**

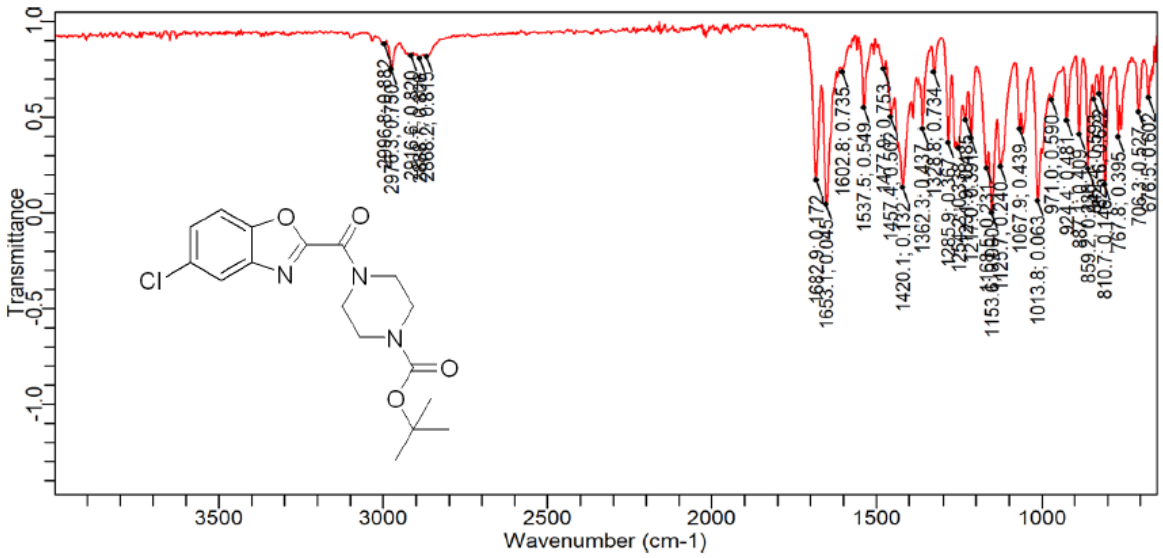


**Figure 26:** IR of compound **6.**

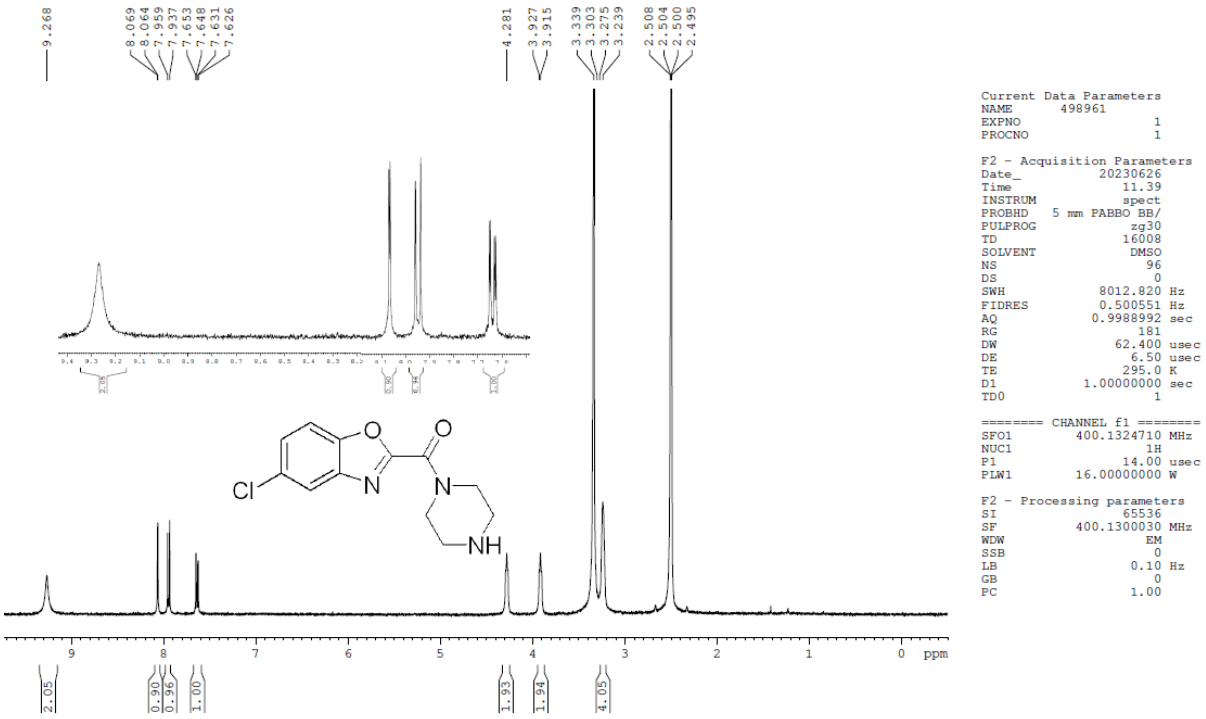


**Figure 27:** $^{1}$H NMR of compound **7.**

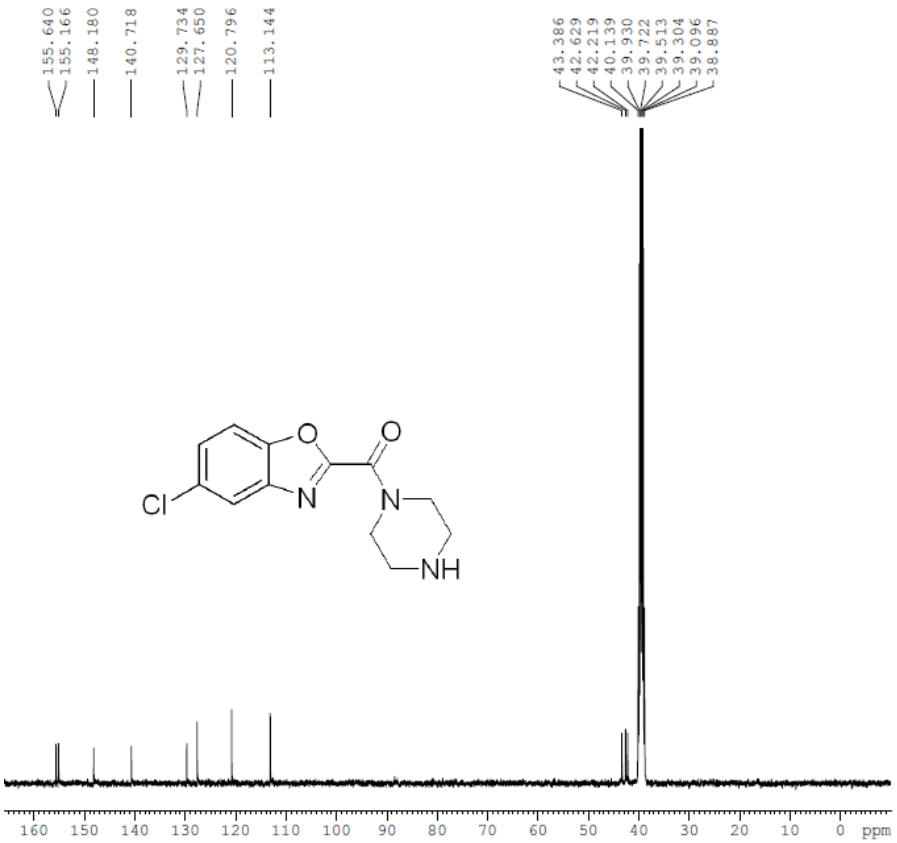


```
Current Data Parameters
NAME       611123
EXPNO           1
PROCNO          1

F2 - Acquisition Parameters
Date_      20231004
Time          12.39
INSTRUM       spect
PROBHD  5 mm PABBO BB/
PULPROG     zgpg30
TD           65536
SOLVENT       DMSO
NS            1024
DS               4
SWH       24038.461 Hz
FIDRES        0.366798 Hz
AQ            1.3631488 sec
RG              203
DW             20.800 usec
DE              6.50 usec
TE             296.9 K
D1        2.00000000 sec
D11       0.03000000 sec
TD0             1

======== CHANNEL f1 ========
SFO1      100.6228293 MHz
NUC1            13C
P1             10.00 usec
PLW1      53.95100021 W

======== CHANNEL f2 ========
SFO2      400.1316005 MHz
NUC2            1H
CPDPRG[2     waltz16
PCPD2          90.00 usec
PLW2      16.00000000 W
PLW12      0.38716000 W
PLW13      0.31360000 W

F2 - Processing parameters
SI              32768
SF        100.6128160 MHz
WDW               EM
SSB       0
LB             2.00 Hz
GB        0
PC             1.40
```

**Figure 28:** $^{13}$C NMR of compound **7.**

| | | | |
|---|---|---|---|
| Sample Name: | *Amine intermidiate* | | |
| Sample Type: | Unknown | Acquired By: | LCMS-02 |
| Vial: | 2:D,7 | Sample Set Name: | 30062023 UCH 183 2nd |
| Injection #: | 1 | Acq. Method Set: | METHOD C3 |
| Injection Volume: | 0.70 ul | Processing Method: | METHOD_C3, METHOD_C3_02 |
| Run Time: | 3.0 Minutes | Channel Name: | 230.0nm, MS TIC, 290.0nm |
| Project Name | LCMS-02_JUNE-2023_30062023 | Proc. Chnl. Descr.: | PDA 290.0 nm Blank Subtracted |
| Date Acquired: | 30-06-2023 21:26:11 IST | | |
| Date Processed: | 01-07-2023 01:33:21 IST, 01-07-2023 01:33:29 IST, 01-07-2023 01:33:40 IST | | |

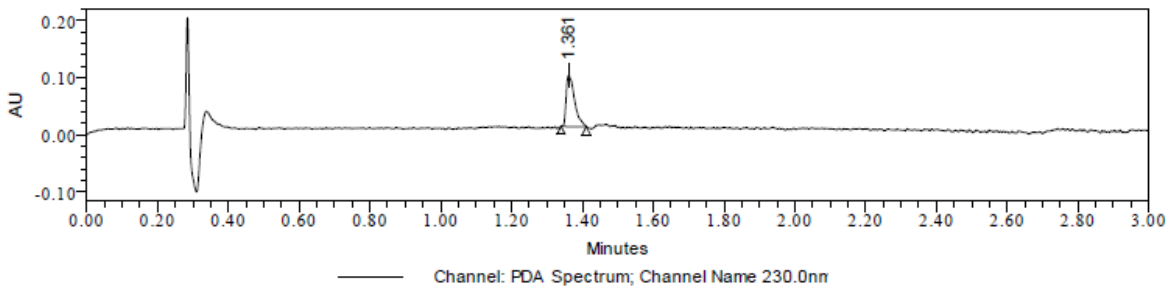

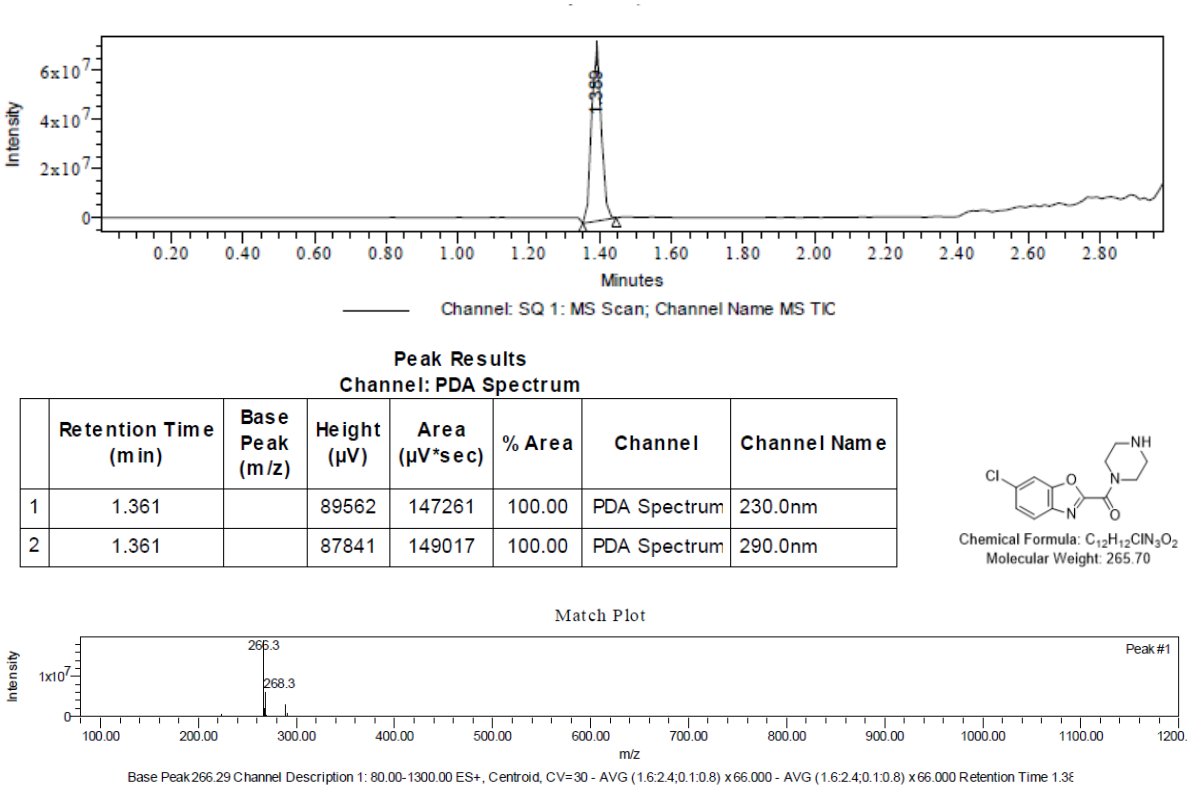


**Figure 29:** LC-MS of compound **7.**

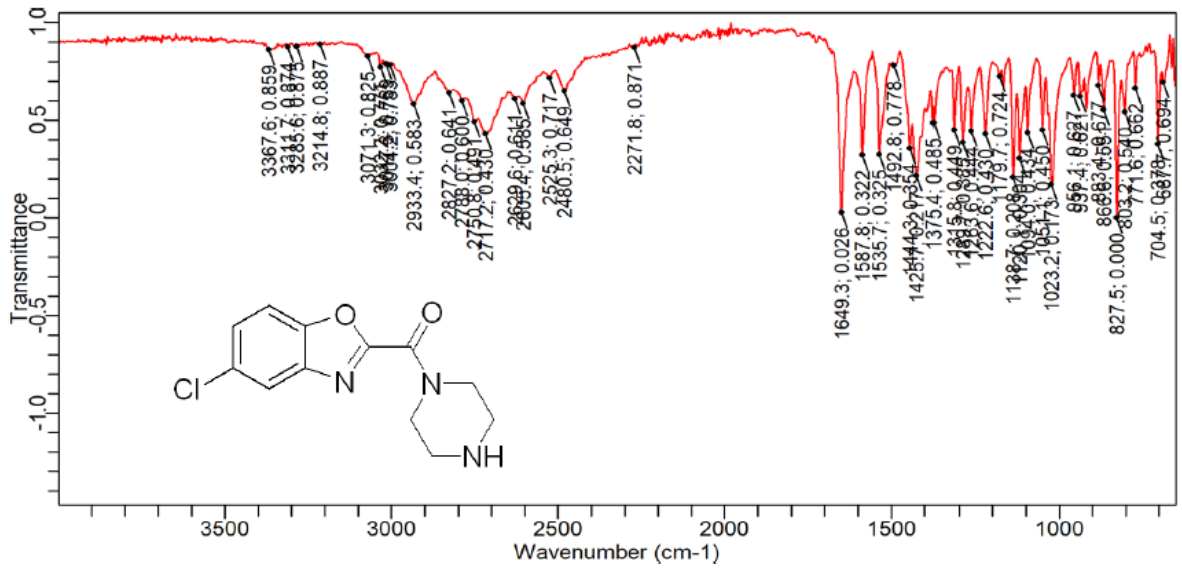


**Figure 30:** IR of compound **7.**

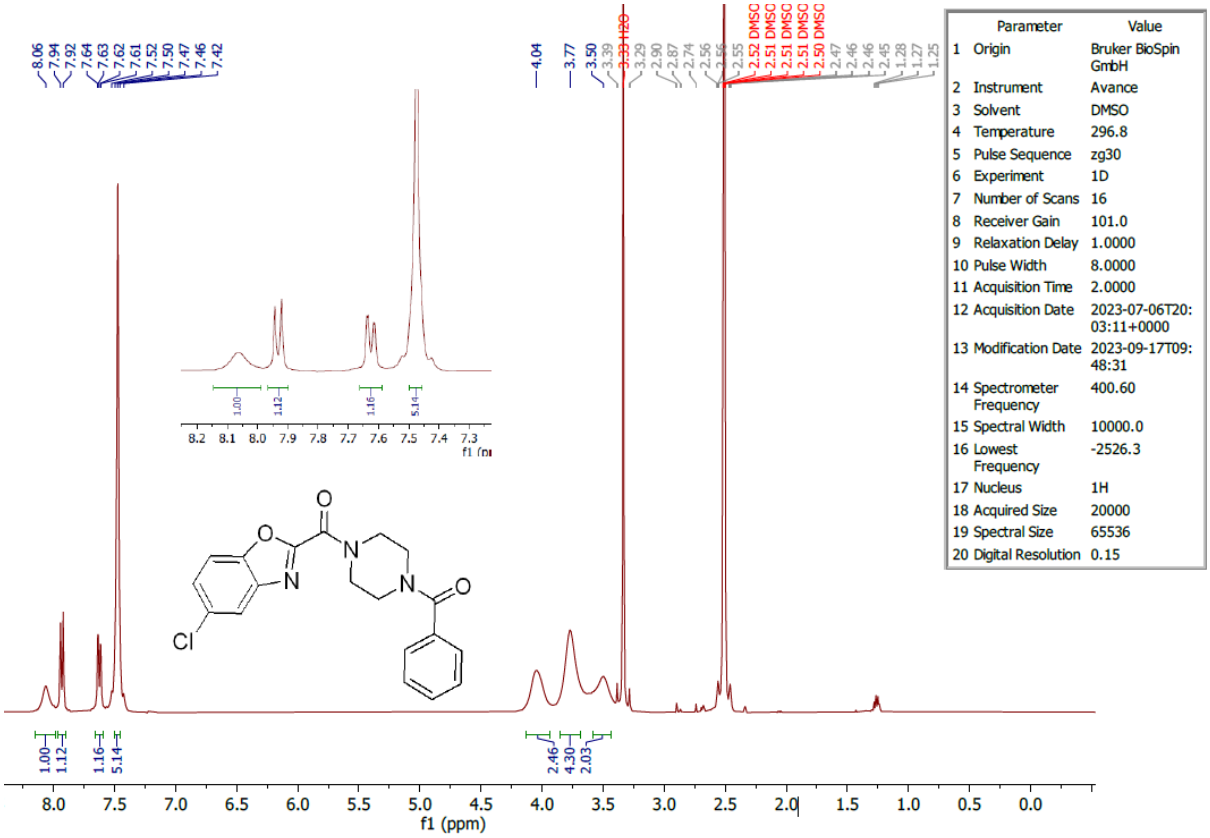


**Figure 31:** $^{1}$H NMR of compound **9a.**

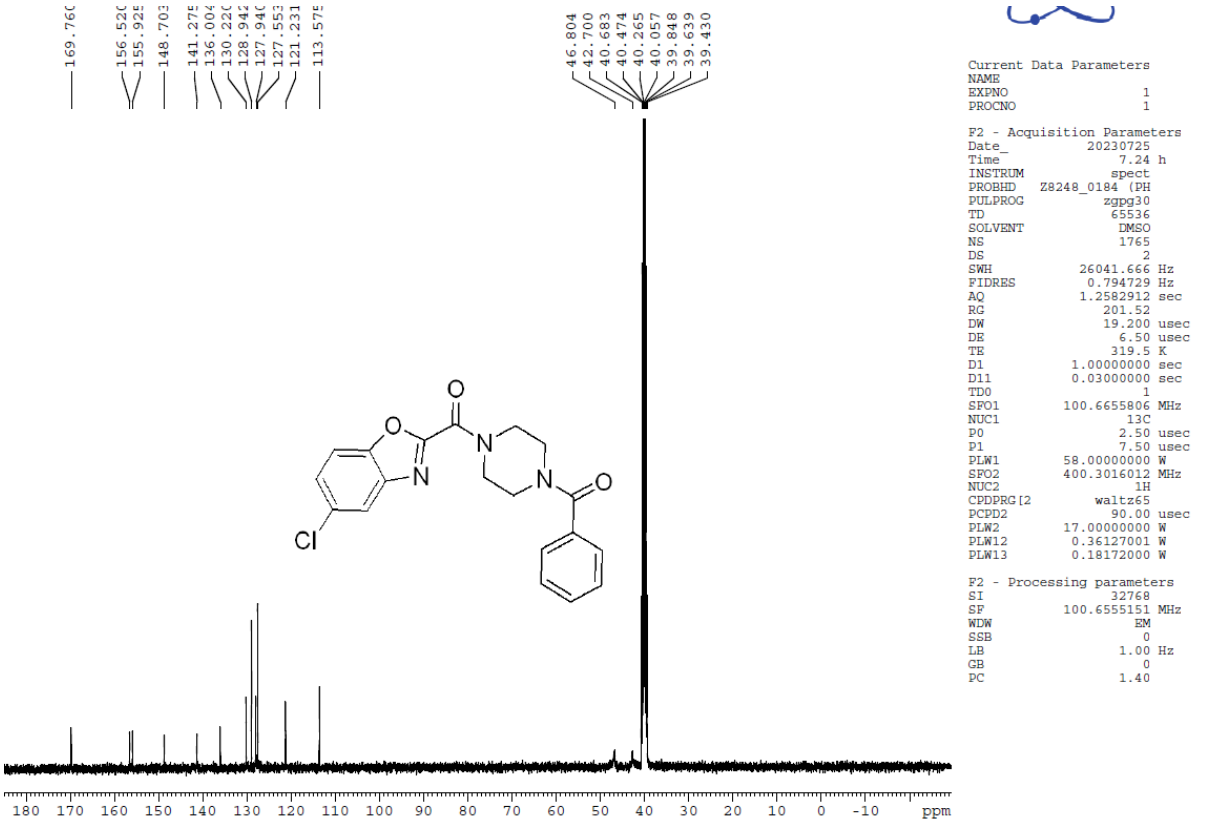


**Figure 32:** $^{13}$C NMR of compound **9a.**

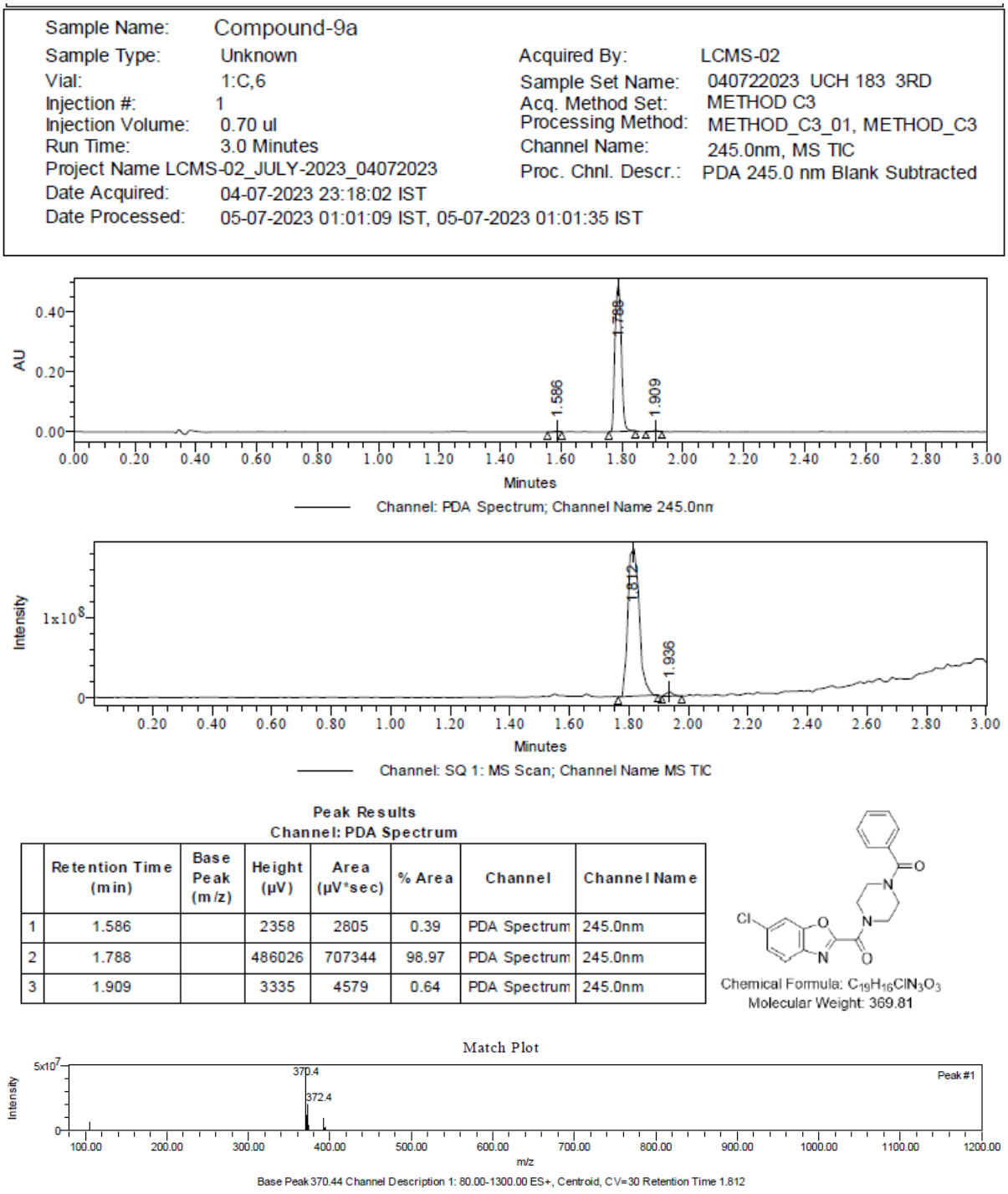


| | Retention Time (min) | Base Peak (m/z) | Height (µV) | Area (µV*sec) | % Area | Channel | Channel Name |
|---|---|---|---|---|---|---|---|
| 1 | 1.586 | | 2358 | 2805 | 0.39 | PDA Spectrum | 245.0nm |
| 2 | 1.788 | | 486026 | 707344 | 98.97 | PDA Spectrum | 245.0nm |
| 3 | 1.909 | | 3335 | 4579 | 0.64 | PDA Spectrum | 245.0nm |

**Figure 33:** LC-MS of compound **9a.**

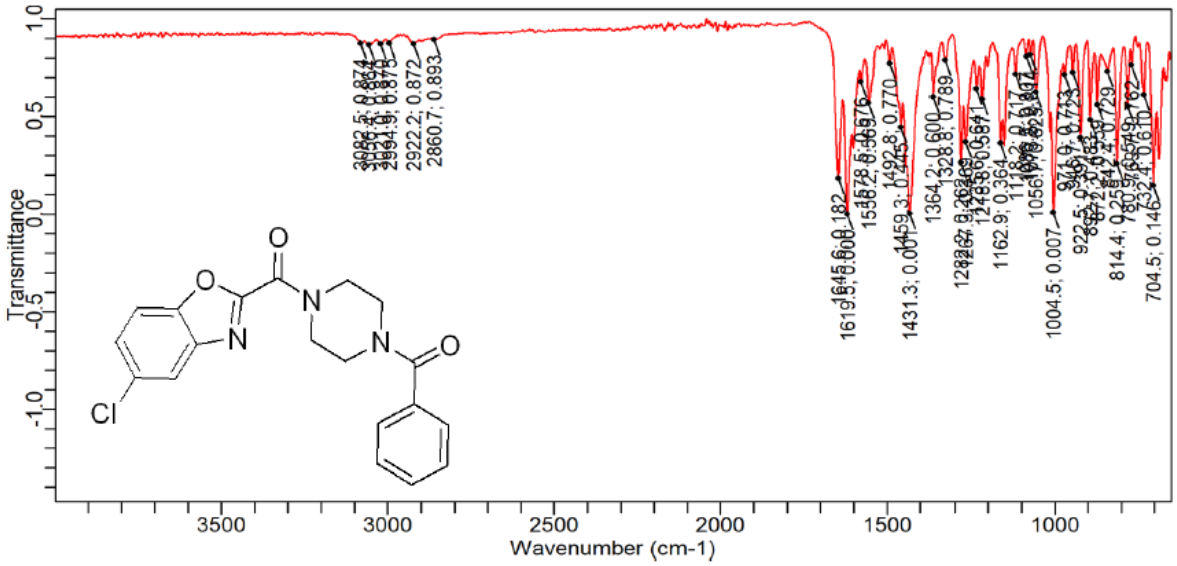


**Figure 34:** IR of compound **9a.**

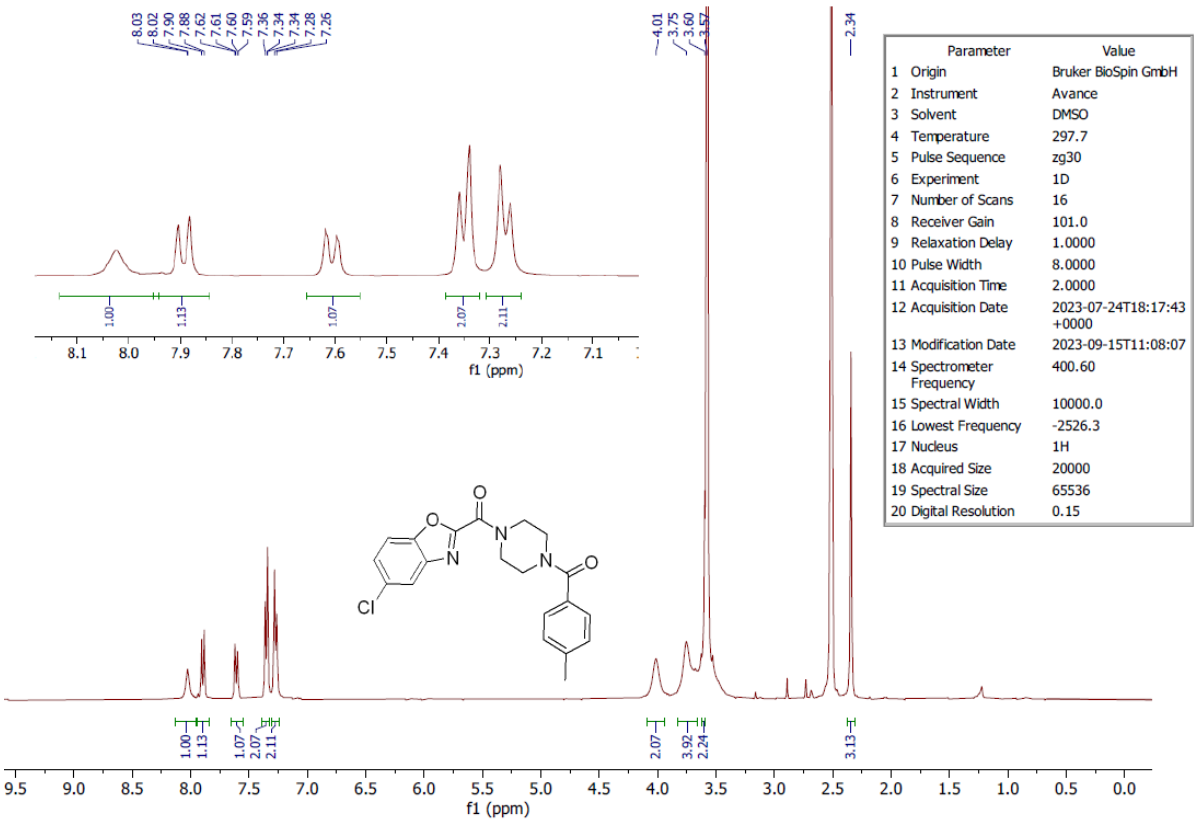


**Figure 35:** $^{1}$H NMR of compound **9b.**

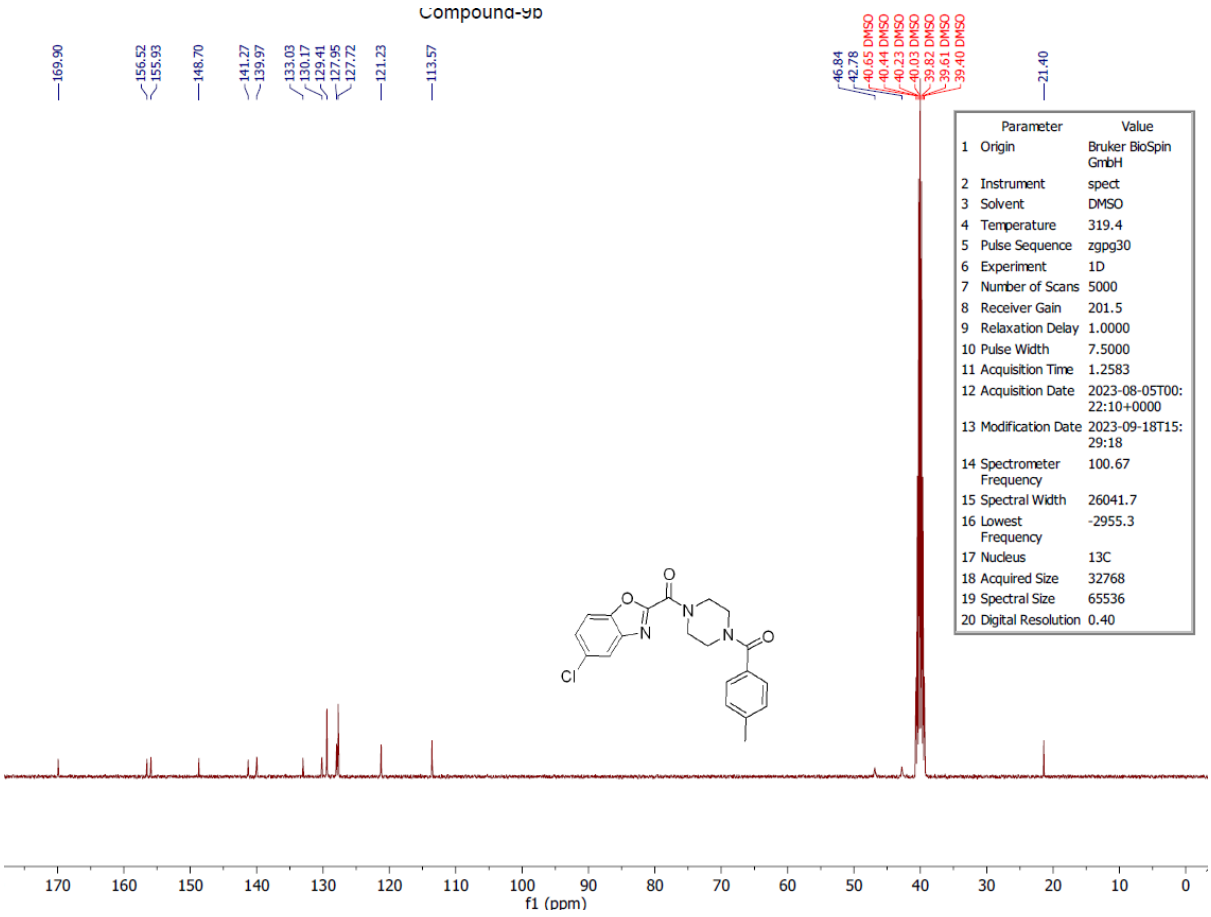


**Figure 36:** $^{13}$C NMR of compound **9b.**

| | | | |
|---|---|---|---|
| Sample Name: | Compound-9b | | |
| Sample Type: | Unknown | Acquired By: | LCMS-02 |
| Vial: | 1:B,5 | Sample Set Name: | 11072023_UCH 183_NIGHT |
| Injection #: | 1 | Acq. Method Set: | METHOD C3 |
| Injection Volume: | 1.00 ul | Processing Method: | METHOD_C3 01, METHOD_C3 |
| Run Time: | 3.0 Minutes | Channel Name: | 245.0nm, MS TIC, 210.0nm |
| Project Name | LCMS-02_JULY-2023_11072023 | Proc. Chnl. Descr.: | PDA 245.0 nm Blank Subtracted |
| Date Acquired: | 12-07-2023 00:01:57 IST | | |
| Date Processed: | 12-07-2023 03:13:37 IST, 12-07-2023 03:13:48 IST, 12-07-2023 03:14:05 IST | | |

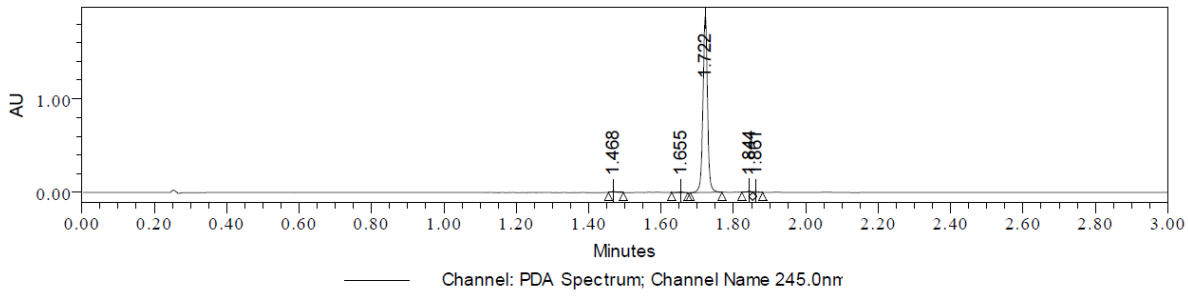

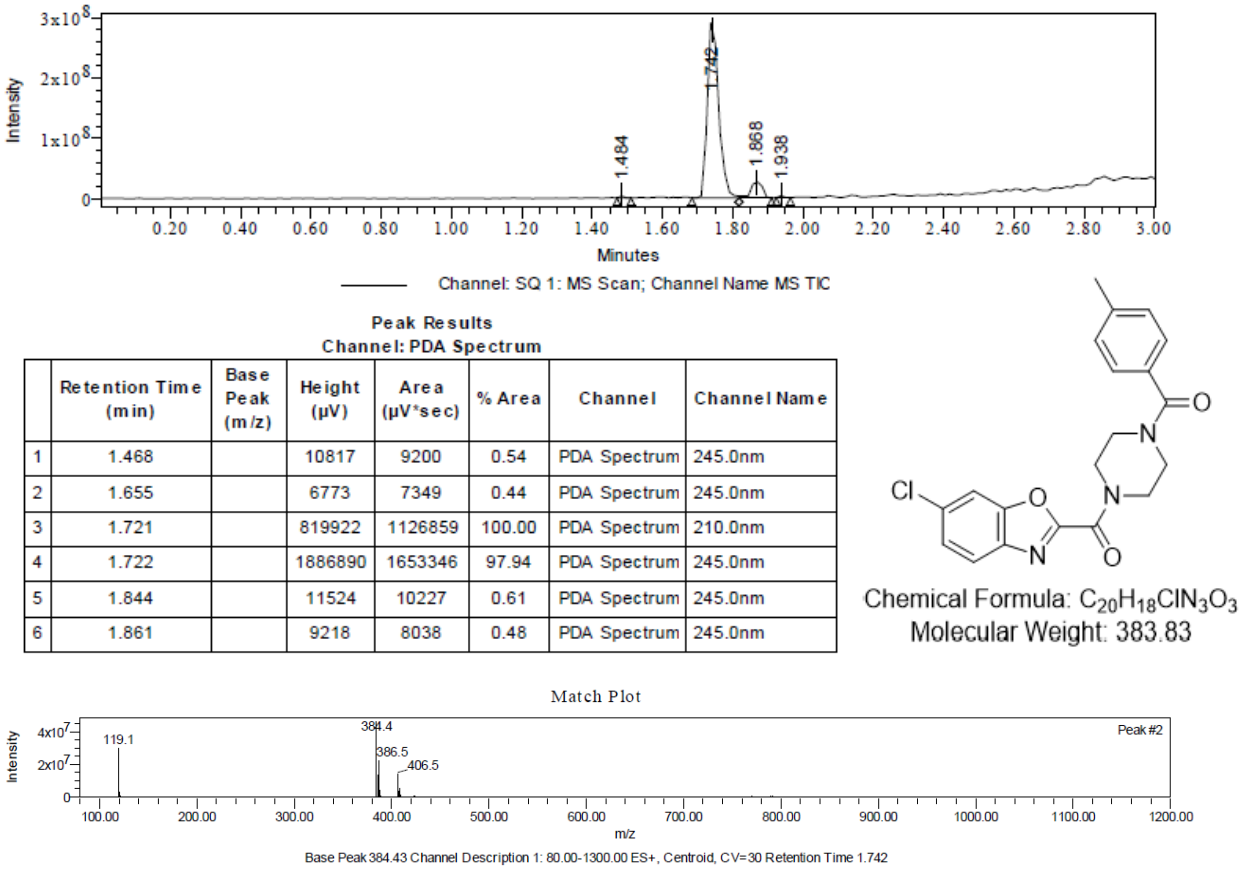


| | Retention Time (min) | Base Peak (m/z) | Height (µV) | Area (µV*sec) | % Area | Channel | Channel Name |
|---|---|---|---|---|---|---|---|
| 1 | 1.468 | | 10817 | 9200 | 0.54 | PDA Spectrum | 245.0nm |
| 2 | 1.655 | | 6773 | 7349 | 0.44 | PDA Spectrum | 245.0nm |
| 3 | 1.721 | | 819922 | 1126859 | 100.00 | PDA Spectrum | 210.0nm |
| 4 | 1.722 | | 1886890 | 1653346 | 97.94 | PDA Spectrum | 245.0nm |
| 5 | 1.844 | | 11524 | 10227 | 0.61 | PDA Spectrum | 245.0nm |
| 6 | 1.861 | | 9218 | 8038 | 0.48 | PDA Spectrum | 245.0nm |

**Figure 37:** LC-MS of compound **9b.**

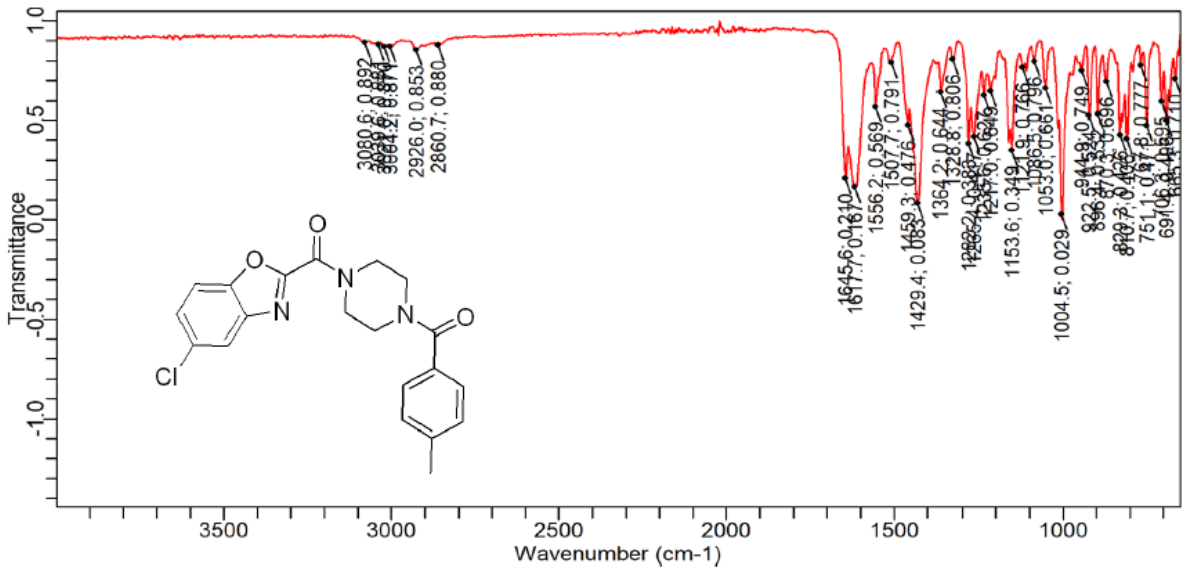


**Figure 38:** IR of compound **9b.**

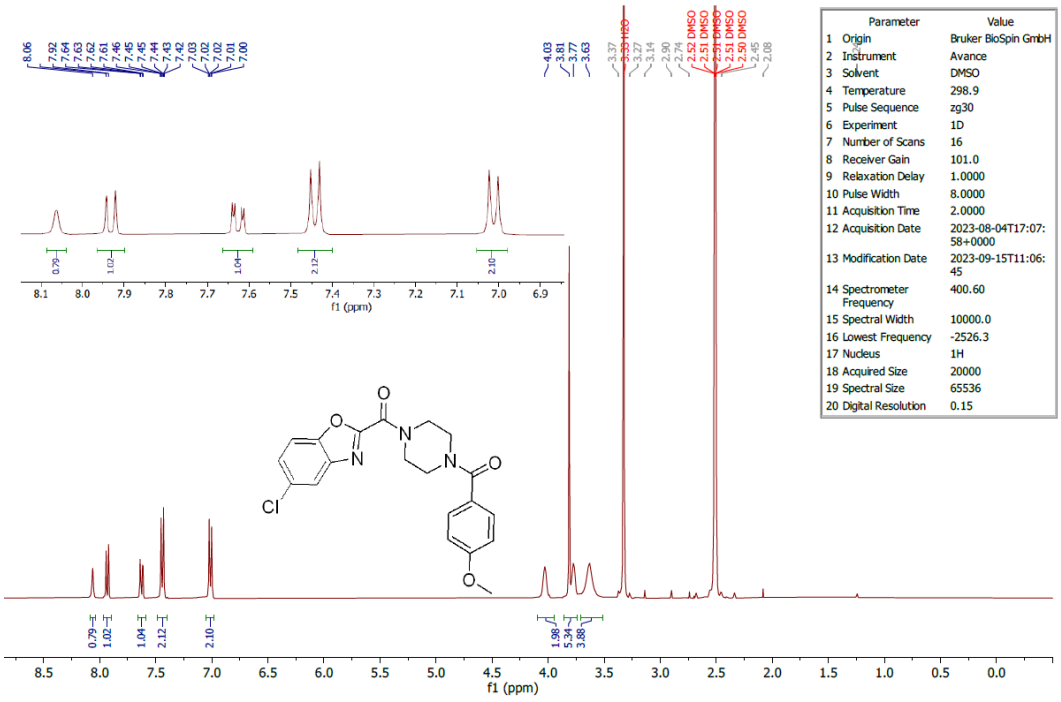


**Figure 39:** $^{1}$H NMR of compound **9c.**

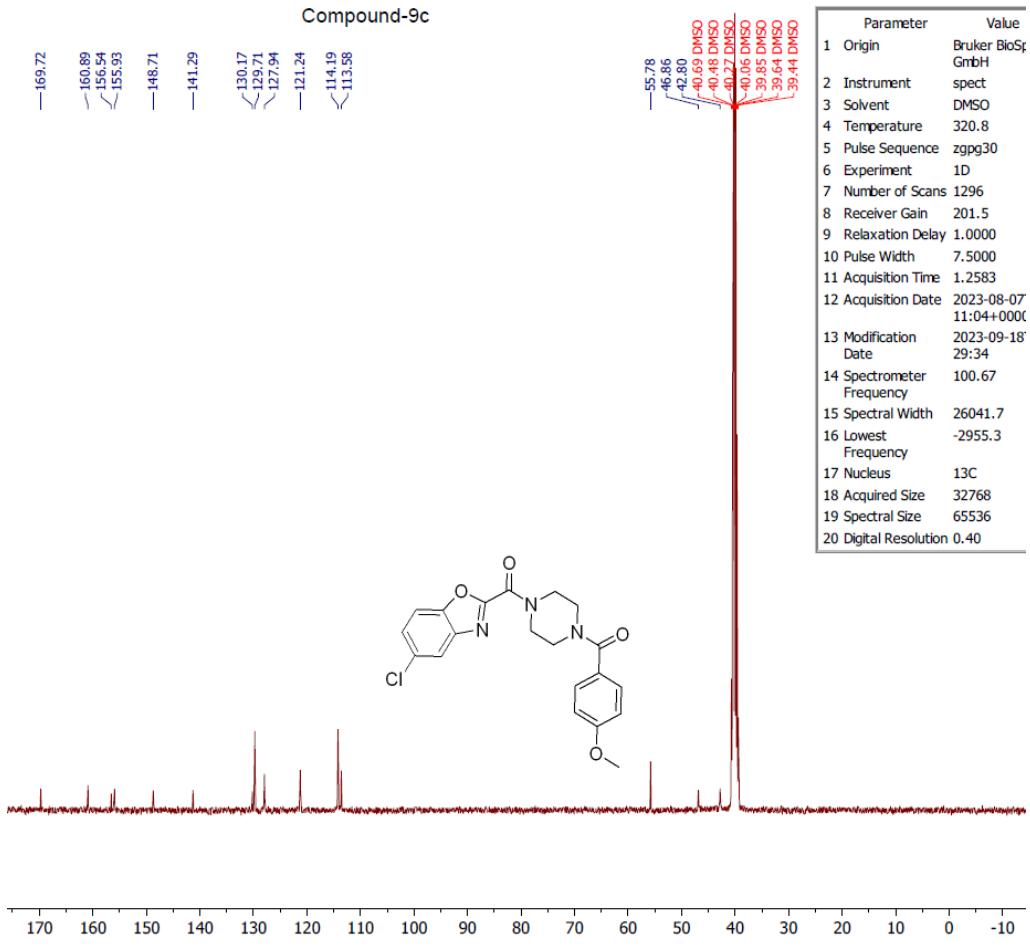


**Figure 40:** $^{13}$C NMR of compound **9c.**

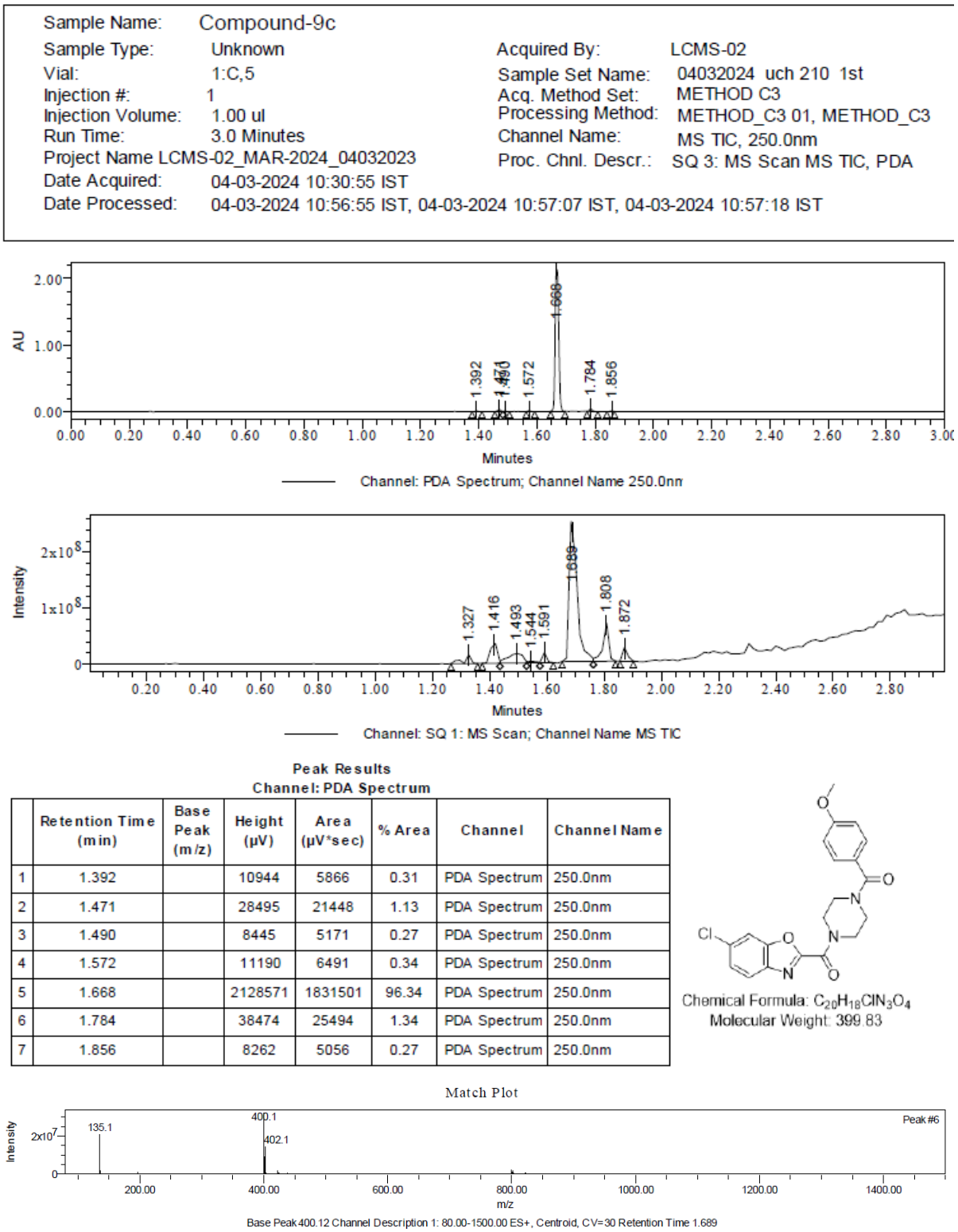


| | Retention Time (min) | Base Peak (m/z) | Height (µV) | Area (µV*sec) | % Area | Channel | Channel Name |
|---|---|---|---|---|---|---|---|
| 1 | 1.392 | | 10944 | 5866 | 0.31 | PDA Spectrum | 250.0nm |
| 2 | 1.471 | | 28495 | 21448 | 1.13 | PDA Spectrum | 250.0nm |
| 3 | 1.490 | | 8445 | 5171 | 0.27 | PDA Spectrum | 250.0nm |
| 4 | 1.572 | | 11190 | 6491 | 0.34 | PDA Spectrum | 250.0nm |
| 5 | 1.668 | | 2128571 | 1831501 | 96.34 | PDA Spectrum | 250.0nm |
| 6 | 1.784 | | 38474 | 25494 | 1.34 | PDA Spectrum | 250.0nm |
| 7 | 1.856 | | 8262 | 5056 | 0.27 | PDA Spectrum | 250.0nm |

**Figure 41:** LC-MS of compound **9c.**

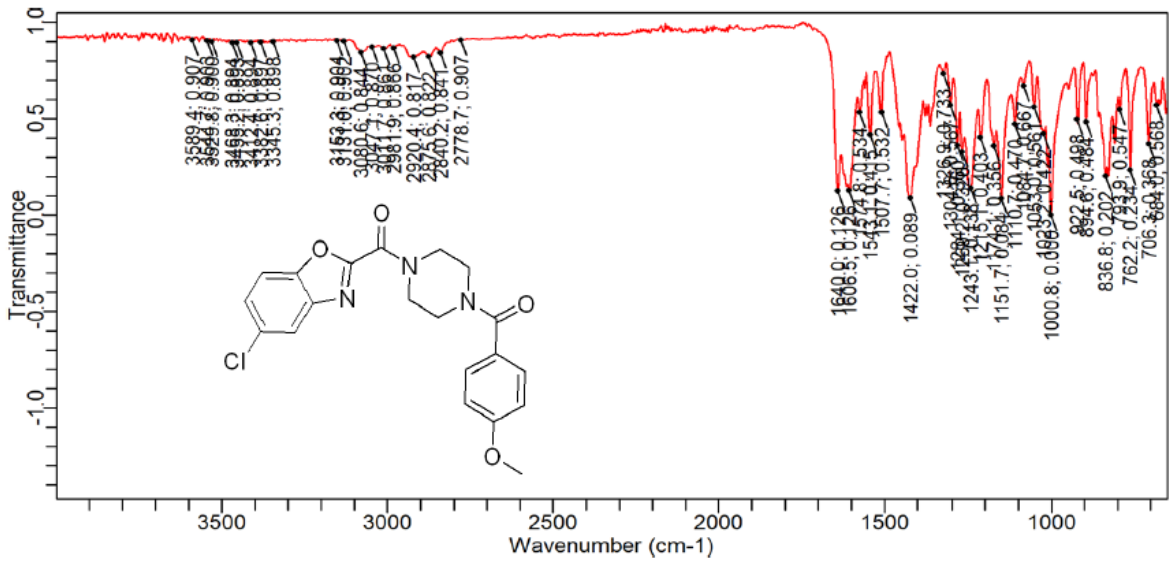


**Figure 42:** IR of compound **9c.**

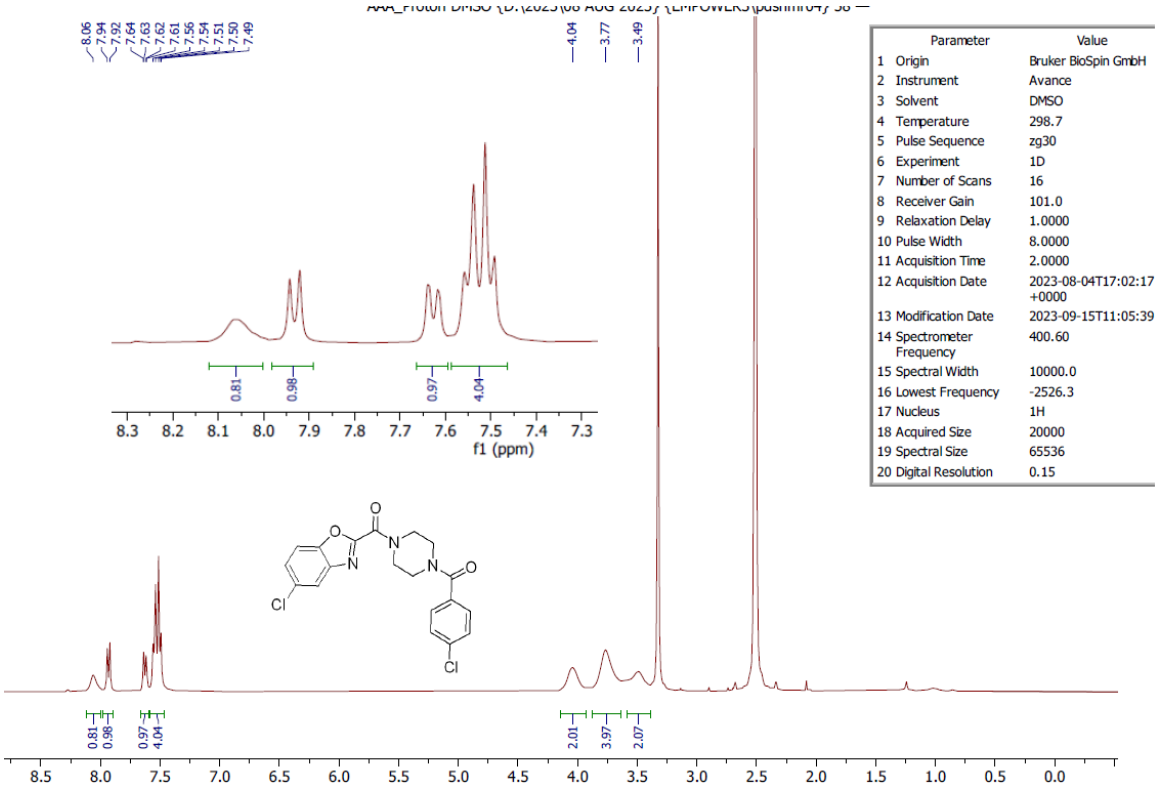


**Figure 43:** $^{1}$H NMR of compound **9e.**

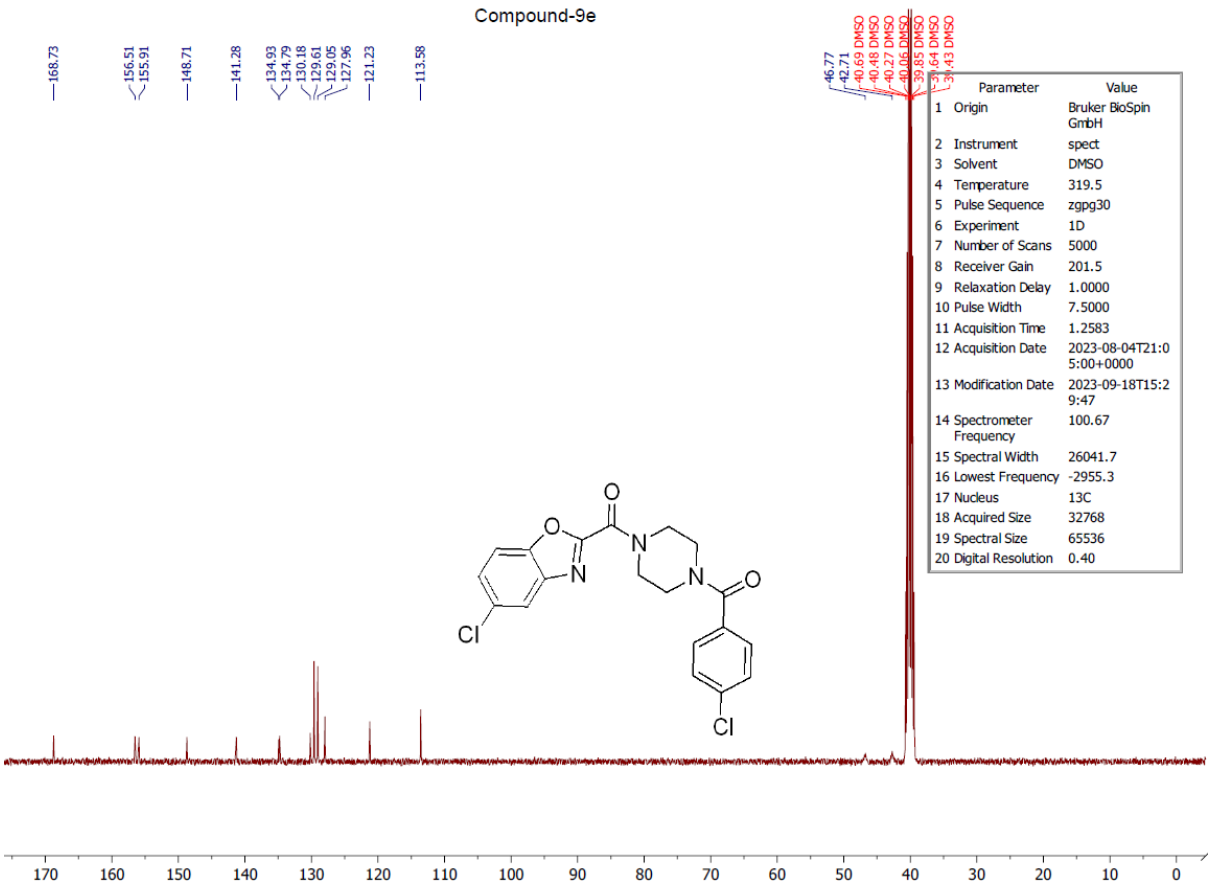


**Figure 44:** $^{13}$C NMR of compound **9e.**

| | | | |
|---|---|---|---|
| Sample Name: | Compound-9e | | |
| Sample Type: | Unknown | Acquired By: | LCMS-02 |
| Vial: | 1:B,4 | Sample Set Name: | 11072023_UCH 183_NIGHT |
| Injection #: | 1 | Acq. Method Set: | METHOD C3 |
| Injection Volume: | 1.00 ul | Processing Method: | METHOD_C3 01, METHOD_C3 |
| Run Time: | 3.0 Minutes | Channel Name: | 220.0nm, MS TIC, 265.0nm |
| Project Name | LCMS-02_JULY-2023_11072023 | Proc. Chnl. Descr.: | PDA 265.0 nm Blank Subtracted |
| Date Acquired: | 11-07-2023 23:57:53 IST | | |
| Date Processed: | 12-07-2023 03:06:41 IST, 12-07-2023 03:07:02 IST, 12-07-2023 03:07:18 IST | | |

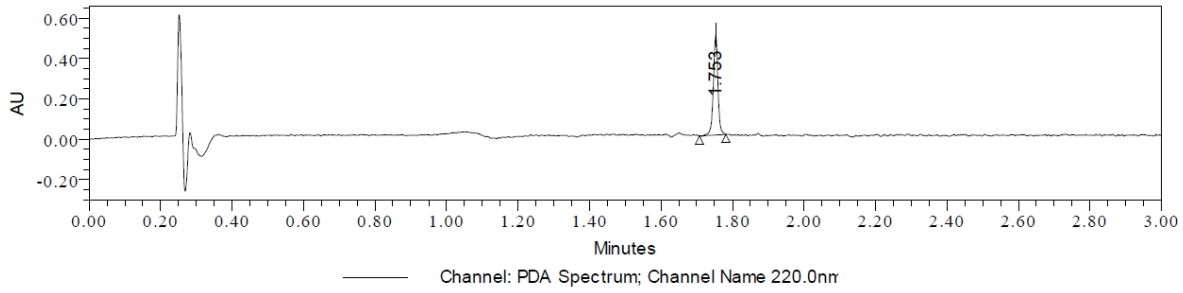

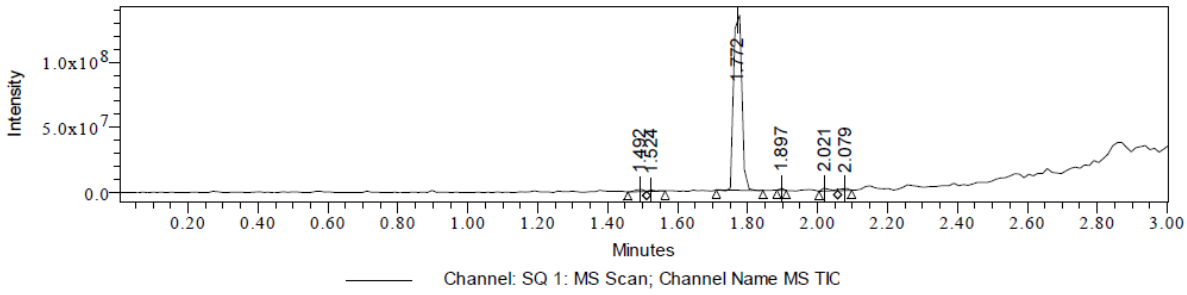


**Peak Results**
**Channel: PDA Spectrum**

| | Retention Time (min) | Base Peak (m/z) | Height (µV) | Area (µV*sec) | % Area | Channel | Channel Name |
|---|---|---|---|---|---|---|---|
| 1 | 1.469 | | 2183 | 1874 | 0.64 | PDA Spectrum | 265.0nm |
| 2 | 1.652 | | 2150 | 2324 | 0.80 | PDA Spectrum | 265.0nm |
| 3 | 1.753 | | 331369 | 283289 | 97.44 | PDA Spectrum | 265.0nm |
| 4 | 1.753 | | 496740 | 441578 | 100.00 | PDA Spectrum | 220.0nm |
| 5 | 1.876 | | 2866 | 2624 | 0.90 | PDA Spectrum | 265.0nm |
| 6 | 1.902 | | 997 | 618 | 0.21 | PDA Spectrum | 265.0nm |

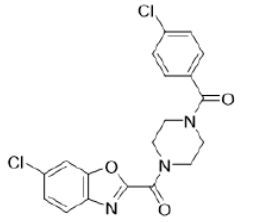


Chemical Formula: $C_{19}H_{15}Cl_2N_3O_3$
Molecular Weight: 404.25

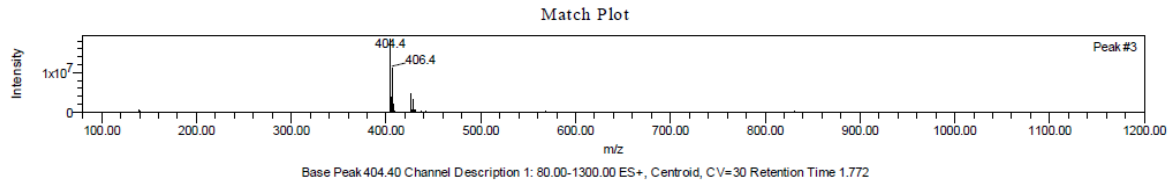


**Figure 45:** LC-MS of compound **9e.**

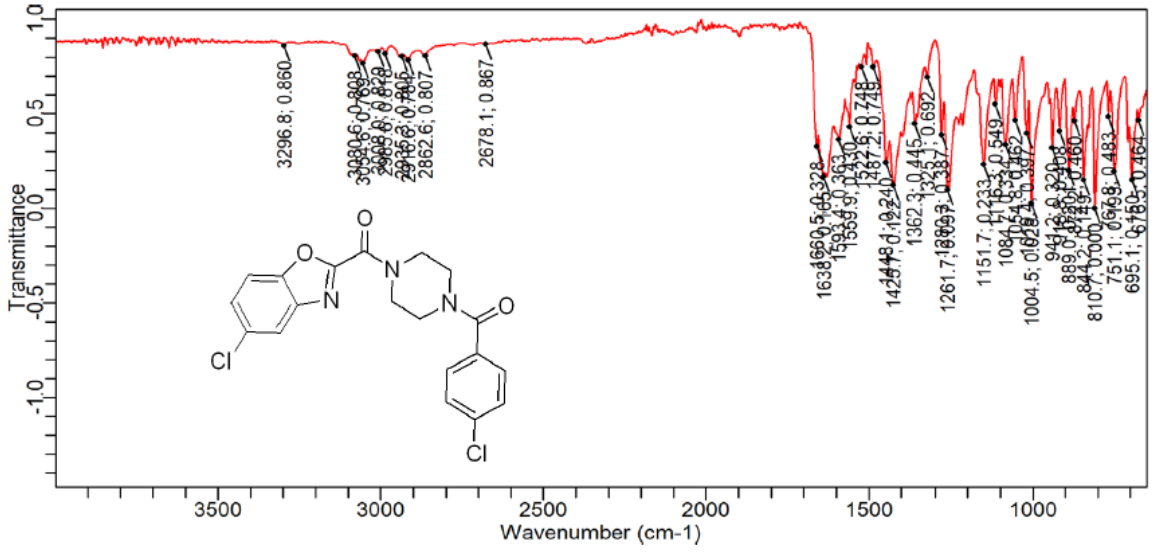


**Figure 46:** IR of compound **9e.**

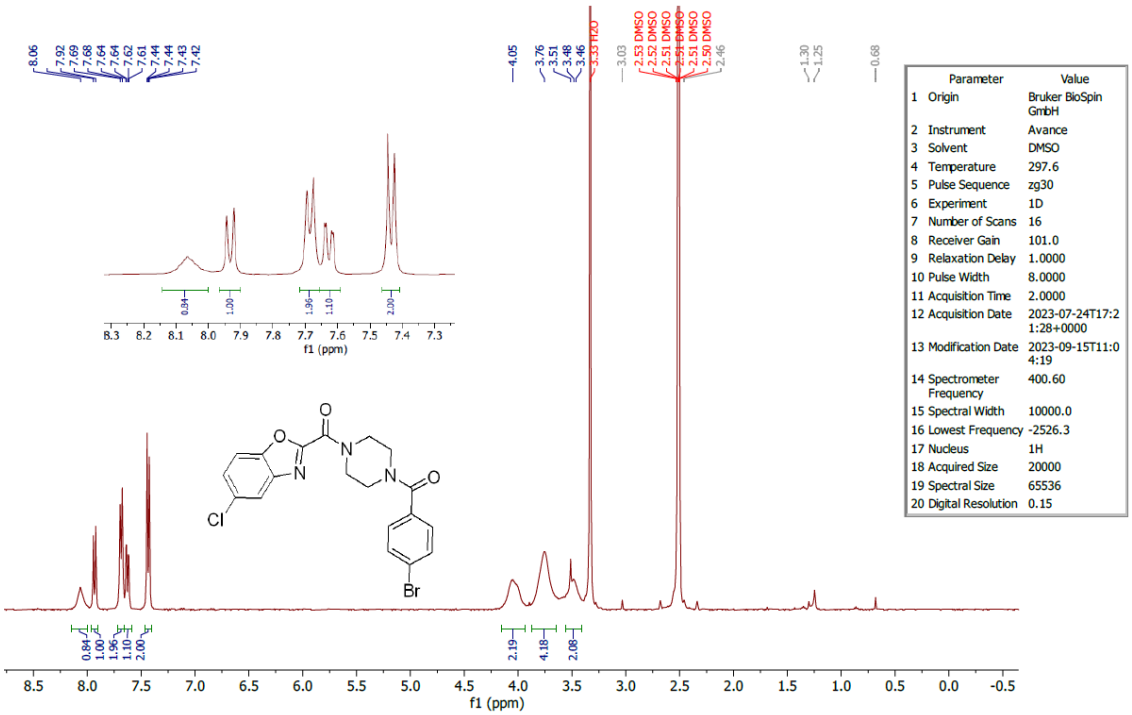


**Figure 47:** $^{1}$H NMR of compound **9f.**

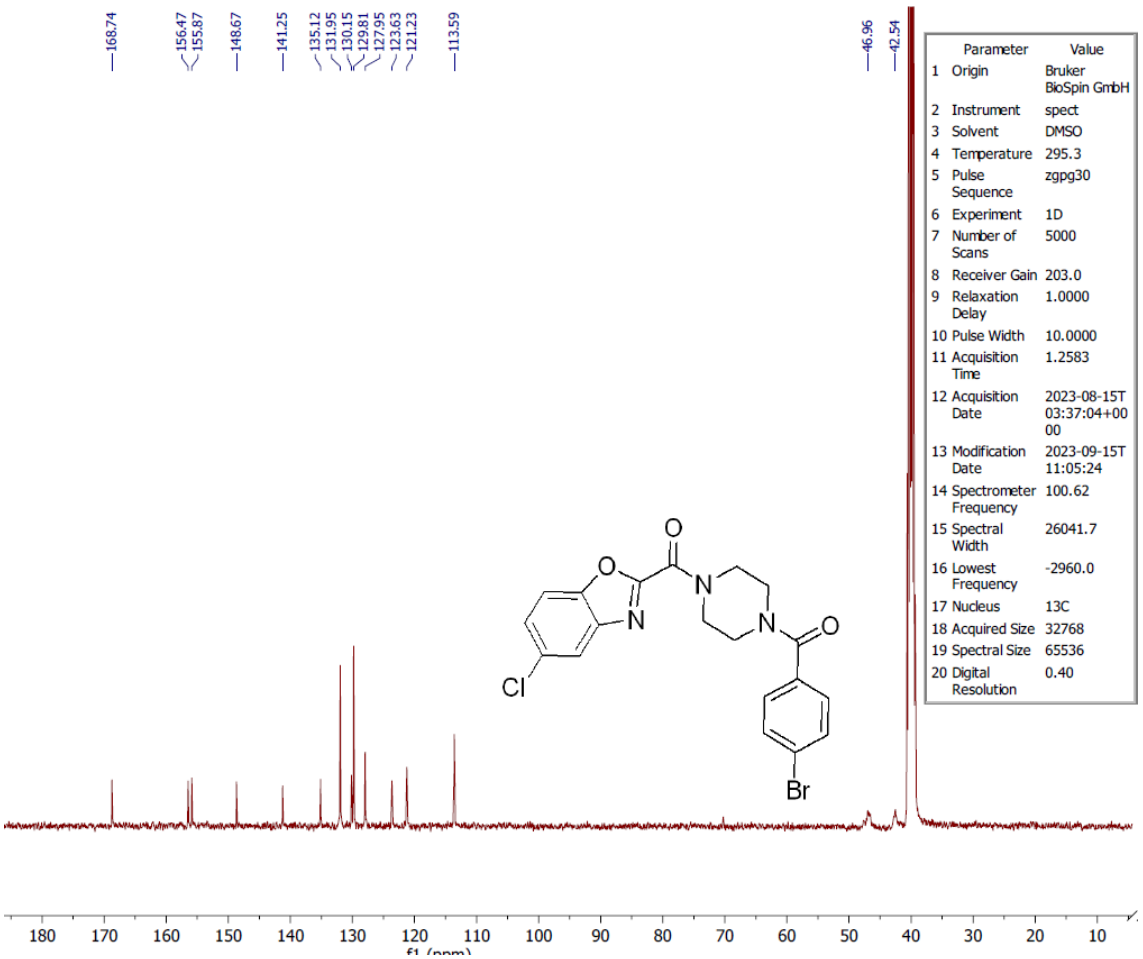


**Figure 48:** $^{13}$C NMR of compound **9f.**

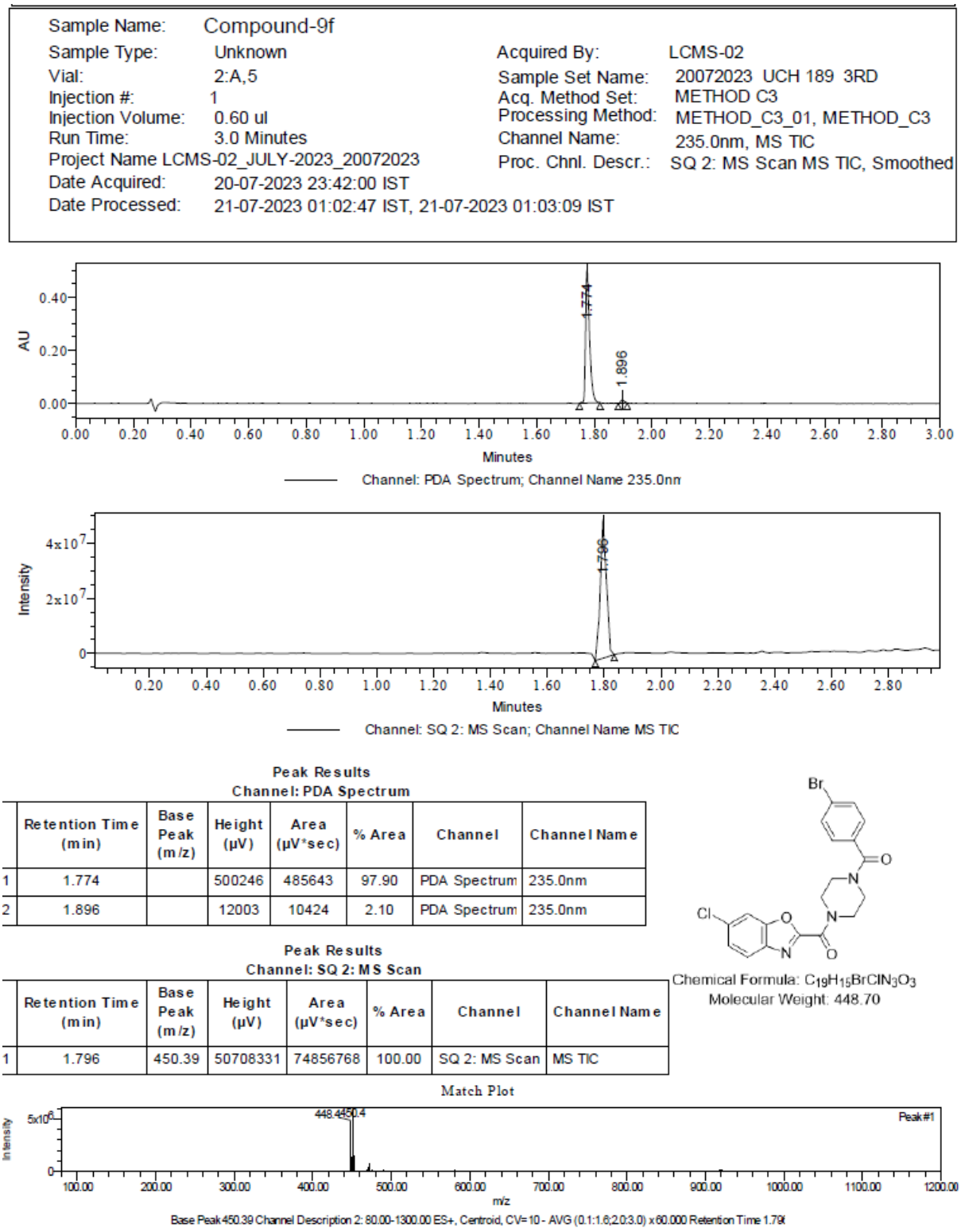


**Figure 49:** LC-MS of compound **9f.**

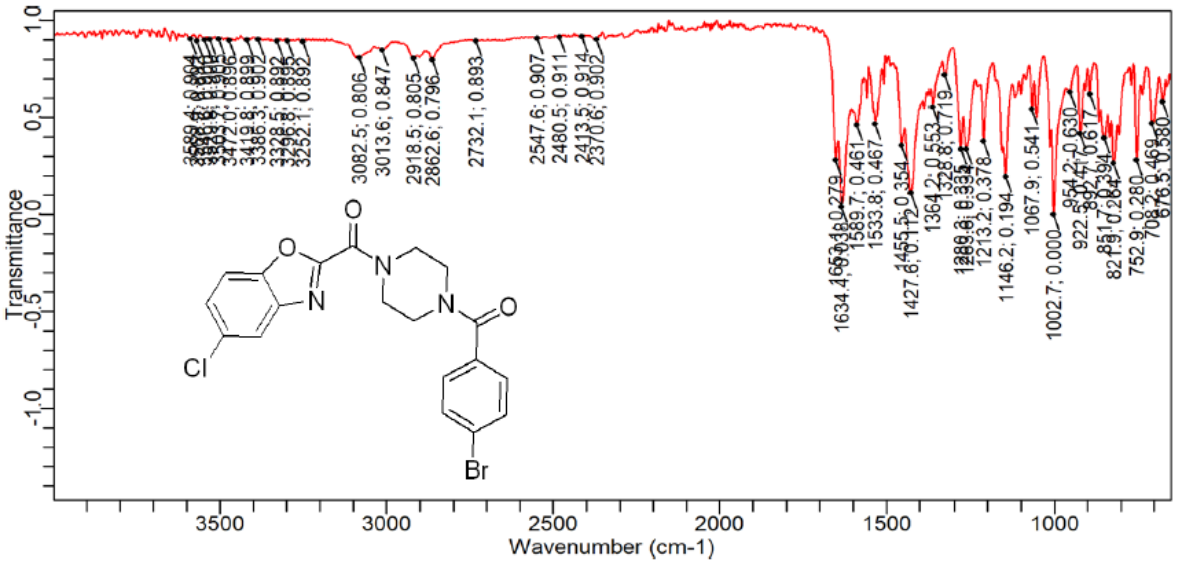


**Figure 50:** IR of compound **9f.**